Single-molecule Fluorescence Imaging Techniques

Dylan A. Reid and Eli Rothenberg

New York University School of Medicine, New York, NY, USA

The past decade has been witnessed to exciting developments in advanced fluorescence microscopy techniques that rely on visualizing single emitting fluorophores. The proliferation of single-molecule fluorescent imaging techniques and their application in biological research have the potential to revolutionize how research is performed and greatly increase our understanding of biological systems. Presently, these techniques are still relatively niche owing to technological barriers, but it is foreseeable that they will become an increasingly common way in which insights are sought in biology. Here, we review the basic principles of key single-molecule techniques and their recent biological applications.

1 INTRODUCTION

The light microscope is one of the oldest tools employed by biologists, offering a glimpse of cellular events invisible to the naked eye. Throughout its long history, light microscopy implemented important technological advancements that retained its prominence in biological research. One of the most important changes to occur in microscopy was the adoption of fluorescent labels to aid in imaging in biological samples. Fluorescence is a physical phenomenon where a molecule is able to absorb a photon of a specific wavelength and emit a photon of a longer wavelength. In this manner, a target of interest to a biologist might be labeled by a fluorescent molecule, probed with one wavelength of light, and the emission of the fluorescence collected while rejecting all other light. Specific labeling of biomolecules in this manner opens up the possibility to study their behaviors in greater depth. The use of fluorescent labels in biology has also been greatly enhanced by the development of specific labeling strategies, such as fluorescently tagged antibodies and genetically encoded fluorescent protein tags.[1,2] These opened new opportunities for biological research and further established the central role of fluorescence-based techniques and assays in biological research.

The biological sciences have relied heavily on ensemble measurements reporting average characteristics, with the average band in a gel containing billions of molecules or the average fluorescent foci containing thousands of molecules. However, averages mask the underlying complexity inherent in biological systems. Over the past decade, fluorescence microscopy has undergone a revolution through the development of new techniques, which circumvent many of the limitations of conventional

Encyclopedia of Analytical Chemistry, Online © 2006–2015 John Wiley & Sons, Ltd.

This article was published in the *Encyclopedia of Analytical Chemistry* in 2015 by John Wiley & Sons, Ltd.
DOI: 10.1002/9780470027318.a9494

optical microscopy. These techniques are collectively referred to as single-molecule techniques and rely on the visualization of single emitting fluorophores in order to make inferences about the biological systems in questions. By observing single molecules, the heterogeneity of a system becomes visible. Early single-molecule fluorescence experiments in the early 1980s involved the direct observation of individual DNA molecules stained with the nucleic acid-specific dyes.[3,4] Now, advances in the technology since these early days allow for the visualization of single-dye molecules, enabling the study of complex biochemical or cellular processes.[5–8]

Here we describe several leading single-molecule fluorescence imaging techniques, which have been widely applied in the past decade. Following the basic principles of each technique, we will review some of the biological problems it has been used to address.

2 TECHNICAL CONSIDERATIONS FOR SINGLE-MOLECULE TECHNIQUES

Single-molecule methods and assays remain highly specialized and challenging, requiring dedicated instruments and a breadth of skills including optics, photophysics, fluorescence spectroscopy, computer programming, and specific assay development. The majority of these methods were developed in physical science laboratories, using customized instruments, dedicated computers and software interfaces, and highly tailored data analysis computer programs.[9] The increasing interest of the biomedical research community in single-molecule and super-resolution microscopy methods has encouraged microscopy companies to develop microscopy systems with integrated single-molecule capabilities. These commercial microscopy systems provide an impressive array of imaging modalities, but they are extremely costly, especially as compared to in-house customized systems or standard commercial microscopy systems.[10]

It is important to emphasize that single-molecule imaging capabilities alone, as delivered by these systems, do not address the many fundamental aspects of single-molecule microscopy experiments, including assays development, sample preparation, determining the appropriate imaging settings, troubleshooting, and data analysis. These features must be established as an integral part of the experimental technique before the actual measurements.

On the other hand, the availability of several detailed tutorials and guides on single-molecule techniques, including step-by-step assays and troubleshooting, and instrumentation development offer an affordable and approachable alternative to scientists with an aptitude for tweaking instruments and a do-it-yourself (DIY) approach. In this section, we provide a condensed overview of the central components in a custom-built single-molecule systems. We direct the readers to the following references for a more in-depth reading.[11–15]

2.1 Microscopy Systems and Objective Lens

A single-molecule system can be customized around most manual inverted fluorescence microscopy systems. These systems typically have two ports; one port for coupling the excitation source onto the sample and the other port for the detector that measures the light being emitted from the sample.

The central most important component of a bare fluorescence microscope is its objective lens, which determines the collection efficiency of light emitted from the sample. The objective lens is particularly important in single-molecule microscopy as every photon that is collected from the sample improves the precision of the measurement. The collection efficiency of an objective is measured by its numerical aperture (NA), with high NA corresponds to higher collection efficiency.[16] The NA varies with the working distance, the distance between the objective and the focus, and medium of the objective lens; air objective having the longest working distance with the highest NA of 0.9, water immersion objectives with shorter working distance and NA of 1.3, and oil immersion objective with NA of 1.4–1.6. It is important to note that while objective lenses with high magnification typically have high NA, magnification is secondary to NA, so that an objective with 60× magnification and NA of 1.46 would perform better than an objective with 100× magnification and NA of 1.2.

2.2 Detectors

To detect photons emitted from individual molecules, highly sensitive detectors are required. The initial single-molecule experiments utilized point detectors such as photomultiplier tubes (PMTs) and avalanche photo diodes (APDs), or array detectors such as high quantum efficiency charge couple device (QE-CCD) cameras, liquid nitrogen-cooled charge couple devices (CCDs), and intensified charge couple devices (ICCDs).[17–20] While these detectors were capable of detecting photons emitted from individual molecules, they came with a daunting price tag and had some considerable limitation such as detection efficiency, dynamic range, dark noise, and acquisition rates. The proliferation of the semiconductor industry along with various technological innovations over the past two decades resulted in much improved and affordable CCD detectors. Electron multiplying charge

Encyclopedia of Analytical Chemistry, Online © 2006–2015 John Wiley & Sons, Ltd.

This article was published in the *Encyclopedia of Analytical Chemistry* in 2015 by John Wiley & Sons, Ltd.
DOI: 10.1002/9780470027318.a9494

couple device (EMCCD) cameras began to be utilized for single-molecule detection about 10 years ago, providing superior thermocooling (−70 to −100 °C), extremely low dark noise, and high quantum efficiency (∼95%), which afford photon counting capabilities.[21] These cameras transformed single-molecule microscopy, enabling the development of new single-molecule methods, and supported further improvement in existing methods. In recent years, new scientific complementary metal-oxide semiconductor (sCMOS) cameras were utilized in single-molecule microscopy.[22] These sCMOS cameras are less sensitive than EMCCD cameras, but present reasonable single-molecule detection capabilities and have more pixels and faster frame rates than EMCCD camera.[23,24]

2.3 Mode of Illuminations and Excitation Sources

Single-molecule microscopy often uses lasers as excitation sources. Lasers have a narrow well-defined emission wavelength and a collimated light beam. These features enable to control the sample's mode of illumination and provide excellent separation of the excitation and emission bands as compared to standard arc lamp excitation sources. In standard epifluorescence microscopes, the excitation light propagates through the sample resulting in out-of-plane signal, which can distort and mask the signal coming from the sample's plane.[25] An important advantage of using lasers for sample excitation in single-molecule experiments is the ability to modify their mode of illumination to reduce sample's background and increase the overall signal-to-noise ratio (S/N). This is achieved using total internal reflection fluorescence (TIRF) illumination mode.[26] In this scheme, the majority of the laser's light does not penetrate the sample and reflects back, and only a little fraction of the light known as an evanescent field propagates into the sample. The evanescent field does not propagate through the sample but exponentially decays, leading to an effective excitation profile of ∼100 nm above the coverslips surface.[27] This enables the selective illumination and excitation of molecules that are closed to the surface, such as surface-tethered molecules and membranes of adherent cells.[28−31] It is important to note that the TIRF does not improve the axial (z-axis) resolution of a microscopy system, but limits the excitation profile and improves the S/N. The axial resolution is defined as the ability to resolve two adjacent objects in the axial dimension and depends only on the emission wavelength and NA.[32,33]

There are two common ways to achieve TIRF excitation, through a prism or through an objective, as illustrated Figure 1.[34] Prism-based TIRF typically uses a four-sided Pellin–Broca prism, placed on the top glass surface of the sample's perfusion chamber.[13] A laser

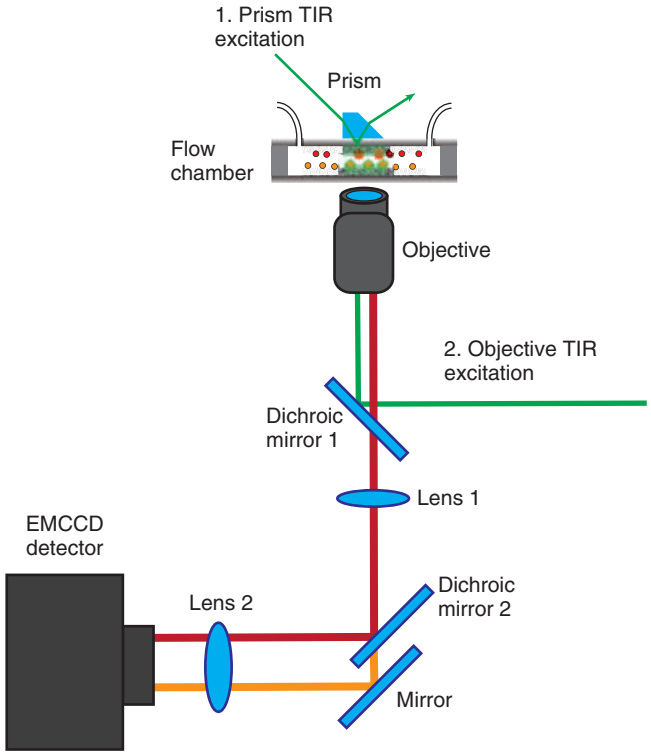

Figure 1 Diagram of a TIRF microscopy system. In the case of Prism TIR excitation (1), the inverted microscope has an objective focusing on the slide side of the mounted flow cell. A prism rests on this slide and an excitation laser is aimed through the prism and slide to the critical TIR angle between the glass and water interface. A dichroic filter rejects excitation light, while emission is collected in this case and split into two different channels on a single EMCCD detector. In the case of objective TIR excitation (2), an excitation laser is aimed through the back aperture of a high NA oil objective until the critical angle is reached to generate TIR between the glass and water interface. The same objective collects the emitted fluorescence split into two channels on an EMCCD detector.

is sent onto the prism results in TIR and evanescent field on the surface farther from the objective lens. The emission from the sample is typically collected using a high NA water immersion objective having a long working distance, enabling it to collect light from the opposite surface. In objective-based TIRF, the same objective lens is used to generate the TIRF and collect the light emitted from the sample.[34] To generate TIRF using an objective, a laser beam is first expanded and then focused on the back aperture of a high NA (better than 1.4) oil immersion objective. Positioning the focused laser beam closer to the rim of the objective's back aperture will result in total internal reflection (TIR), whereas positioning the laser in the center of the back aperture will generate regular epifluorescence illumination. The link between the position of the laser on the back aperture

Encyclopedia of Analytical Chemistry, Online © 2006–2015 John Wiley & Sons, Ltd.

This article was published in the *Encyclopedia of Analytical Chemistry* in 2015 by John Wiley & Sons, Ltd.
DOI: 10.1002/9780470027318.a9494

and the resulting mode of illumination can be further utilized in selective sample illumination. For instance, positioning the laser closer to the rim, but not in TIR mode, results in highly inclined illumination (sometimes referred to as HILO or light sheet illumination) that enables excitation deeper in the sample beyond TIR penetration limits, but with improved S/N as compared to regular epifluorescence, as the laser is refracted sideways and does not propagate through the sample.[35−37]

3 SINGLE-MOLECULE FLUORESCENCE RESONANCE ENERGY TRANSFER

3.1 Principle of Forster Resonance Energy Transfer

FRET (Forster resonance energy transfer) is a fluorescence spectroscopy and microscopy method that has been widely applied in various fields, including biological studies, material sciences, and photophysics.[38] The underlining principle of FRET is a distance-dependent interaction between a pair of different dye molecules known as the FRET pair. This interaction involves the direct excitation of one donor molecule (D) and the emission from the other acceptor molecule (A) and arises from a dipole–dipole interaction between the two fluorophores (D–A).[39,40] Being strongly distance dependent, FRET is sometimes referred to as a 'spectroscopic ruler'.[41] The functional form of the distance dependence of the FRET efficiency is expressed as (Equation 1)

$$E_{\mathrm{FRET}} = \frac{1}{(1 + (R/R_0)^6)} \tag{1}$$

where E_{FRET} is the FRET efficiency, R the distance between the two fluorophores, and R_0 a coefficient representing a number of physical factors that govern the dipole–dipole interaction, such as quantum-yield and orientation and strength of the transition dipole moment.[39] The effective distance for FRET interaction of a standard FRET pair is between 2 and 8 nm, providing an excellent tool for probing distance changes in bimolecular systems.[42−44] To measure changes in the FRET efficiency, the emission intensities of the donor and acceptor are spectrally resolved and recorded.[45] The FRET efficiency can then be found through the relationship (Equation 2):

$$E_{\mathrm{FRET}} = \frac{I_{\mathrm{Acceptor}}}{(I_{\mathrm{Acceptor}} + I_{\mathrm{Donor}})} \tag{2}$$

where $I_{\mathrm{Acceptor\ (Donor)}}$ is the emission intensity of the Acceptor (Donor). At large D–A separation, a strong Donor emission is observed, along with a weak (or no) emission from the Acceptor. At smaller D–A separation, the Donor emission will decrease while the Acceptor will increase, as more energy is transferred from the donor to the Acceptor, until at very close proximity the Donor emission will dim while the Acceptor strongly emits.

3.2 Single-Molecule Fluorescence Resonance Energy Transfer of Surface-Tethered Samples

The most common approach for single-molecule fluorescence resonance energy transfer (smFRET) experiments is based on microscopes with TIRF illumination, and it requires that molecules of interest be tethered to surface of a flow chamber.[46] The light emitted from these molecules is split into Donor and Acceptors channels and sent onto the two sides of a CCD camera, as illustrated in Figure 1.[47] Diffraction-limited spots corresponding to donor and acceptor molecules are imaged side by side on the EMCCD camera, followed by mapping of the corresponding Donor and Acceptor spots and analysis of their intensities as FRET trajectories (following the dynamics of a FRET pair over time).[47] For tethering the molecules, the surface is first functionalized to suppress nonspecific binding and to enable the tethering of specific functional group. Typically passivation and functionalization are done by coating the surface with inert molecules such as bovine serum albumin (BSA) having a biotin moiety (BSA-biotin), a lipid-bilayer with a fraction of the lipids having a biotin, or polyethylene glycol (PEG) with a fraction of the PEG molecules being biotin-PEG.[13,48] These molecules are then reacted with Streptavidin or NeutrAvidin enabling to specifically tether biotinylated molecules via biotin–streptavidin–biotin linkage.[13]

Following surface passivation molecules having a biotin tag can be directly tethered to the surface. This is illustrated in Figure 2(a), where a four-way DNA junction (Holliday junction) is shown tethered to the surface. These DNA structures undergo rapid structural rearrangements, switching between parallel and antiparallel conformations as a function of salt concentration in the buffer.[42] Images of single molecules corresponding to the Donor and Acceptor, as well as a merge of the two channels, are shown in Figure 2(b). In Figure 2(c), we show a representative trajectory of donor–acceptor intensity and its corresponding FRET trajectory of an individual Holliday junction as it undergoes rapid transitions in FRET corresponding to conformational changes.

Lipid vesicles with biotinylated lipids are also used for tethering in assays where direct surface linkage might affect the activity of the system or for molecules that cannot be tethered or need to be freely moving.[49,50] In this scheme, the vesicles, and not the molecule of

Encyclopedia of Analytical Chemistry, Online © 2006–2015 John Wiley & Sons, Ltd.

This article was published in the *Encyclopedia of Analytical Chemistry* in 2015 by John Wiley & Sons, Ltd.
DOI: 10.1002/9780470027318.a9494

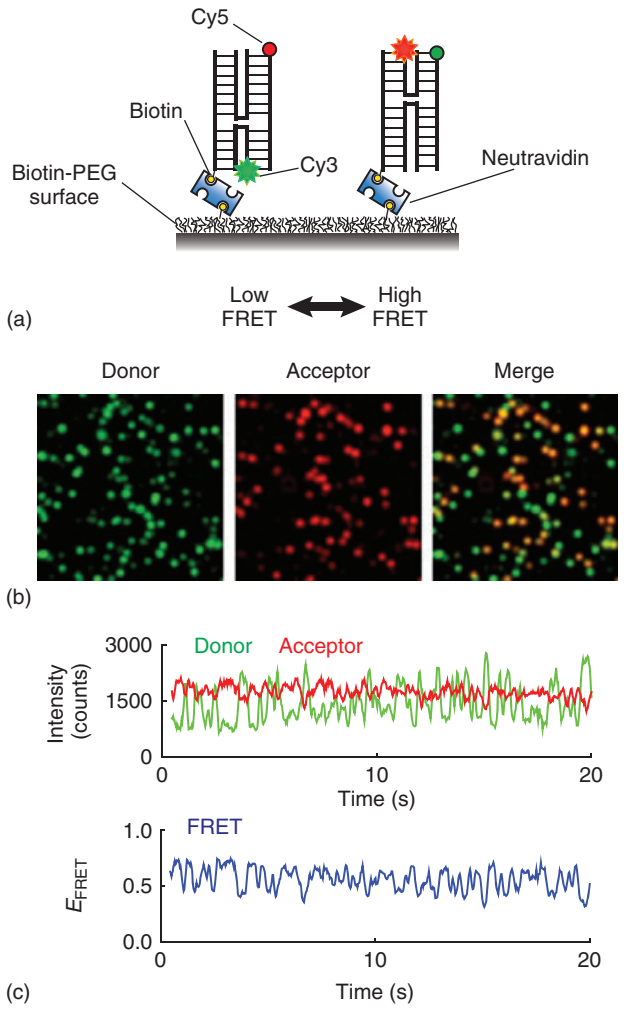

Figure 2 Single-molecule FRET. (a) Cartoon of a Holliday junction DNA substrate attached to a biotin-PEG surface through a neutravidin linker. The DNA is labeled with a Cy3 (Donor) and Cy5 (Acceptor). At certain salt concentrations, the structure interconverts forth between the two displayed structures, corresponding to high and low FRET values. (b) Images of single, diffraction-limited, Cy3- and Cy5-tagged Holliday junctions on a PEG-coated surface in a typical smFRET assay. The Donor and Acceptor channels are shown as a Merge. (c) A typical smFRET trajectory of a Holliday junction alternating conformations. The Donor and Acceptor show alternating intensities, corresponding to the overall changes in FRET efficiency.

interest, are directly tethered to the surface. Vesicles are generated using an extruder setup, and their surface properties and sizes can be varied with precision.[51] Molecules of interest can be either encapsulated inside the vesicles, which have the advantage of greatly increasing the effective concentration of molecules trapped inside vesicles.[49] Proteins may also be incorporated on the surface of vesicles enabling the probing of membrane protein dynamics and vesicles fusion dynamics.[52–54] In addition, proteins such as ion channels can be studied with smFRET in the context of vesicles.[55]

In addition to the surface-tethered smFRET TIRF microscopy assays described earlier, other experimental schemes have been used for smFRET analysis of molecules in solution and away from the surface.[56,57] This approach typically utilizes a microscopy setup where the emission is collected from diffraction-limited confocal excitation volume.[58] The donor and acceptor emissions are separated and each is sent onto a different APD point detector.[19] The resulting signal in these measurements consists of bursts of photons, which are synchronized to determine FRET.[57] This approach does not require the molecules of interest to be tethered and also enable faster acquisition rates for monitoring smFRET events at shorter time scales, but lacks the ability to simultaneously acquire long trajectories of hundreds of molecules as afforded in the TIRF smFRET scheme.

3.3 Long-lived Molecules

A critical obstacle for single-molecule imaging was the rapid photobleaching which individual molecules undergo.[59] This was resolved by introducing oxygen-scavenging systems to the single-molecule imaging buffer.[47] These systems deplete oxygen, which reacts with fluorophores in their excited state. Common oxygen-scavenging systems used in smFRET and other single-molecule experiments are Gloxy (glucose, glucose oxidase, and catalase) and protocatechuate acid (PCA)/protocatechuate-3,4-dioxygenase (PCD).[47,60] Another property of individual fluorophores observed on the single-molecule level is fluorescence intermittency or blinking.[61] This property arises from internal structural changes in dye molecules and is undesirable in smFRET, as it can mask or be interpreted as real FRET changes. To suppress blinking behavior observed on the single-molecule level, β-mercaptoethanol or trolox (6-hydroxy-2,5,7,8-tetramethylchroman-2-carboxylic acid) can be added to imaging buffer.[47,61]

3.4 Analysis

Data analysis is extremely challenging in smFRET experiments, owing in part to the large wealth of data available in single-molecule trajectories. The most straightforward use of smFRET data is simply measuring efficiencies by comparing FRET spots with a control. An example of this would be a DNA helicase assay; an enzyme that unwinds DNA would remove the DNA strand containing the donor molecule, leading to a

Encyclopedia of Analytical Chemistry, Online © 2006–2015 John Wiley & Sons, Ltd.

This article was published in the *Encyclopedia of Analytical Chemistry* in 2015 by John Wiley & Sons, Ltd.
DOI: 10.1002/9780470027318.a9494

loss of FRET with the acceptor strand on the surface. Comparing the relative number of molecules before the helicase is allowed to unwind, with the population following enzyme activity gives a reasonable picture of the molecules efficiency.[62,63] In this manner, a cleverly designed assay can yield results much more quickly than a gel-based assay. Further investigation of smFRET data will examine the trajectories of individual molecules, which can be pooled together to generate FRET histograms.[64] This provides an overall view of the population level of molecules. Histograms provide information about the overall dynamics of the FRET system, hinting at the number of possible FRET states occupied by the molecules. Analysis of individual trajectories yields information about the dwell time and transition rates between different FRET states that are observed in the trajectory and largely depend on the specific behavior of the molecular. Some examples of these behaviors are a single turnover binding or dissociation events, back and forth transitions in a two-state system, or transitions in discrete or continuous multistate systems. Depending on the specific trajectory, characteristics analysis will be done via tedious manual processes and automated procedures such as autocorrelation or cross-correlation analysis, or, when possible, via new analysis algorithms such as hidden Markov modeling, step function fit, and gamma distribution analysis.[65−70]

4 SINGLE-MOLECULE FLUORESCENCE POLARIZATION AND FLUORESCENCE ANISOTROPY

4.1 Principles of Polarization

Fluorescence polarization (FP), also known as fluorescence anisotropy (FA), utilizes the excited state dipole of fluorophores, which have a very distinctive polarized absorption and emission, with preferred absorption of photons polarized at a specific orientation relative to the fluorophores molecular axis, and the emitted photons oriented along a specific axis of the fluorophores.[39] The specific orientation of fluorescent reporters can be resolved by careful analysis of their polarized absorption/excitation and emission properties.[39,71] FA is typically analyzed by separating the fluorescence intensity into its two polarization components (parallel and perpendicular) and monitoring their respective intensities and anisotropy ratio, given by (Equation 3)

$$\text{Anisotropy} = \frac{(I_p - I_s)}{(I_p + 2I_s)} \tag{3}$$

where I_p and I_s are the sample plane parallel (p) and perpendicular (s) polarization components, respectively. The analysis of polarization in fluorescence can be combined with the analysis of polarization in excitation to provide comprehensive mapping of the molecular orientation of the fluorescent reporter. Polarization in excitation is probed by modifying the orientation of a linearly polarized excitation laser while monitoring the resulting intensity changes in the FP components.[72]

FA is particularly useful for probing biological molecules, as tethered fluorescent reporters are excellent sensors for their immediate molecular environment. Changes to a fluorescent reporter's immediate molecular environment typically manifest as an abrupt change in its molecular orientation. FA ensemble assays are widely used to analyze protein–protein interactions, multimerization events, conformation changes, complex association, and cofactor/ligand binding, as these typically are reflected by a change in the restriction of the orientation of fluorescent labeling.[73−75]

4.2 Single-molecule Polarization

Combining FP analysis with single-molecule detection allows resolving new, previously inaccessible, molecular characteristics and providing a powerful platform for biomedical research. Understanding how molecules are rotating in regards to a reference provides unique clues about their modes of action. This is in part due to the large number of molecular machines that have evolved to couple chemical energy into force transduction.[76] Measurement of polarization can be combined with tracking experiments, where rotational movement helps our understanding of mechanic works performed by molecular motors.[77] This approach was utilized to examine the orientation of the light chain of Myosin V examining, which is the lever arm of motor, where motor steps can be correlated with changes in the polarization of the emitting dye, giving clues as to changes in overall orientation.[78−81] Single-molecule polarization experiments were also used in studies of the adenosine triphosphate (ATP) synthase molecular motor, which couples a proton gradient across a membrane into mechanical work, generating ATP from adenosine diphosphate (ADP) and inorganic phosphate.[82,83] Recently, FA was combined with super-resolution microscopy (detailed in the following section) to allow for resolutions well below the diffraction limit of light, with FA contributing enabling to resolve specific information molecular orientation.[84] Although it has yet to receive widespread use, it is likely that it will become an important tool in the assignment of cellular ultrastructure features.

Encyclopedia of Analytical Chemistry, Online © 2006–2015 John Wiley & Sons, Ltd.

This article was published in the *Encyclopedia of Analytical Chemistry* in 2015 by John Wiley & Sons, Ltd.
DOI: 10.1002/9780470027318.a9494

5 SINGLE-MOLECULE LOCALIZATION AND TRACKING

5.1 The Diffraction Limit of Light

Modern light microscopes often operate at the theoretical limits imposed by optics, although in principle, there has been little substantial change in their overall design since the compound microscope of the 1600s. In principle, objective lenses trade increased NA for shortening the focal length of the lens. As mentioned earlier, increased NA also corresponds to immersing the lens in either water or oil to improve the refractive index of the medium to collect more light. This collection of light in modern optical systems is diffraction limited, which was approximated by Ernst Abbe in the 1870s (Equation 4):

$$\text{Abbe's Law} : D = \frac{\lambda}{2\text{NA}} \tag{4}$$

where D is the minimal distance between two adjacent objects where the two can be resolved from one another (and also termed as the resolution of the optical system), λ the wavelength of light, and NA the numerical aperture.[85] This provides the theoretical maximum for all optical systems, including microscopes or radio telescopes (where NA would correspond to the distance between the farthest individual receivers). On the basis of this equation, if one used a high NA objective (1.46) to image a sample with fluorescence at ~500 nm wavelength such as green fluorescent protein (GFP), the maximum resolution that could be obtained is ~171 nm. Even if the collected light is further magnified with expansion lenses, the initial collection limits the information in the signal and magnification would be futile. This physical limit on the information contained in light has only recently been circumvented with clever physical and theoretical techniques.[11,25]

A point source of light, smaller than the diffraction-limited emission, is seen as a point spread function (PSF). Alternatively, it can be referred to as an Airy disc, which is an idealized PSF for a perfect microscopic system. This is the smallest observable feature in a microscope and is how single-fluorescent molecules appear when observed. The initial attempts to circumvent the diffraction limit of single-fluorescent molecules used near-field scanning optical microscopy (NSOM). In NSOM techniques, a fiberoptic probe is scanned over a sample, where the probe tip is significantly smaller than the diffraction limit of light, allowing signal only as the probe scans over the emitting molecule. Lateral resolutions of ~20 nm have been achieved, and z resolutions of ~2 to 5 nm have been reported.[86,87] The primary difficulty of this approach is in the difficulty of instrumentation and convolution and interference effects arising from the edge of the tip.[88,89]

5.2 Single-molecule Localization and Fluorescence Imaging with One Nanometer Accuracy

The next conceptual leap in wide-field microscopy comes from borrowing earlier work in astronomy. Astronomical data actually often resembles single-molecule data, and there is a genuine synergy between the two sciences because many of the same optical problems arise from these data sets. The PSF resembles a 2-D Gaussian function, and finding the peak of the function with a certain certainty is found to be entirely dependent on the signal. This was demonstrated to work for single molecules, leading to the technique FIONA (fluorescence imaging with one nanometer accuracy).[90]

This method is used for tracking single molecules/particles in real time and was initially applied to resolve the step sizes of individual molecular motors. Briefly, the target of interest is labeled with a fluorophore (fluorescent protein, dye molecule, or quantum dot) and imaged, resulting in the detection of diffraction-limited spots on the EMCCD camera. Each diffraction-limited spot is fitted with a 2-D Gaussian curve, which localizes the fluorophore with nanometer accuracy when there is a sufficiently high S/N and enables to localize a single Cy3 molecule to within 2.3 nm and temporal resolution of 30 ms. Nanoscale localization in the z (axial) axis was also demonstrated, and it can be achieved using defocusing or astigmatism approaches.[81,91,92] For defocusing, the emission is a long focal lens that is inserted in the beam path resulting in defocused image with diffraction rings around a central spot, where calibration of the distance between the diffraction ring and the center spot enables to determine the precise location of the object.[81] Astigmatism-based axial localization is achieved by inserting a long focal length cylindrical lens in the emission path. This introduced astigmatism to the PSF that can be calibrated as a function of the axial localization.[93]

FIONA trajectories are analyzed to yield precise quantification of various motion-related factors, such as diffusion coefficients and displacement characteristics.[94−98] These quantifications contain information on the nature of observed motion and its immediate environment, such as directed motion mediated by molecular motors, and free and confined diffusion in the membrane or inside cells. The main advantage of this approach is the ability to observe the motions of proteins and other molecules at their length scales, well below the physical limitations of diffraction-limited microscopy. This approach also is less technologically complex when compared with NSOM and other subdiffraction imaging methods.

There are numerous examples of the use of FIONA and single-molecule tracking to produce significant discovery.

Encyclopedia of Analytical Chemistry, Online © 2006–2015 John Wiley & Sons, Ltd.

This article was published in the *Encyclopedia of Analytical Chemistry* in 2015 by John Wiley & Sons, Ltd.
DOI: 10.1002/9780470027318.a9494

The first of which was its application to determine the step size and processivity of various molecular motors. Initially, this method proved invaluable for understanding the mechanism of walking molecular motors such as Myosin V and Kinesin-1, showing that these proteins walk in a hand-over-hand manner.[90,98,99] FIONA was also used to track motors inside cells enabling to resolve their specific step size.[100,101] More recently, it was applied to the molecular motor, dynein, which determined that it translocates in an uncoordinated manner with both lateral and backwards steps.[102,103] In addition to trafficking and molecular motors, FIONA and single-molecule tracking methods have been applied on a growing variety of biological systems including the study of RNA trafficking in cells.[104] As protein expression is often localized at specific sites, especially in the case of highly polarized cells such as neurons, tracking specific RNAs to their designations and understanding how they arrive are key to the system.[105,106] Additional examples are the study of ribosome dynamics in bacteria, tracking transcription factors, and tracking membrane proteins.[107−113]

6 SINGLE-MOLECULE STOICHIOMETRY

6.1 Counting by Photobleaching

The ability to detect the emission of individual fluorophores enables the counting of the number of molecules contained in a diffraction-limited spot. This is primarily accomplished through analyzing discrete photobleaching events in the intensity trajectories of individual fluorescently labeled complexes; the numbers of photobleaching events are obtained. In this way, if each subunit in a complex is labeled with a single fluorophore, the number of subunits in the complex can be extracted (proportional to the number of photobleaching events observed in the trajectory). This powerful approach was used to analyze the stoichiometry of various complexes including membrane proteins, protein complexes bound to DNA, and RNA components of phage motor subunits.[114−117] Importantly, by utilizing multicolor photobleaching analysis, this approach was also used for the analysis of heterogeneous complexes.[118]

Recently, single-molecule photobleaching was applied to analyze immunoprecipitation products. In this approach, the pulldown target is tethered specifically to the biofunctionalized surface of microfluidics chamber and imaged under the microscope using a tagged target protein that is captured with the specific antitag antibody.[119,120] The pulldown complex can be labeled either endogenously (by fusion to a fluorescent protein) or using fluorescently labeled primary antibody with a dye/antibody ratio of 1 : 1.[119] The fluorescent signal from individual surface-tethered pulldown complexes is analyzed for both colocalization and the number of photobleaching steps to yield the composition and stoichiometry of each target.

In Figure 3, we show an example of photobleaching analysis of DNA damage repair complexes composed of replication protein A (RPA) and DNA repair protein PALB2 that were bound to single-stranded DNA. Here the fluorescently labeled oligonucleotide was immobilized on a coverslip, followed by the addition of RPA. Nuclear extracts containing a second protein, PALB2, are then allowed to bind, and the proteins are labeled with antibodies. Using this approach, we see that PALB2 associates with RPA and are able to gage relative stoichiometries based on the known immunoreactivity of the antibodies used.

6.2 Counting Molecules in Cells

An elegant application of single-molecule counting was its application to determine the stoichiometry and composition of molecular complexes in living cells. Using genetically encoded fluorescent tags, it is possible to perform subunit counting of protein complexes in either fixed or live cells. This was demonstrated with ion channel subunit counting.[121] The primary difficulty in this approach as with normal stoichiometric measurements via photobleaching remains the noise associated with fluorophore emission. However, this can be circumvented by including other fluorescent proteins emitting at different wavelengths.[122] Counting via fluorescent intensity has been used to correlate gene expression and protein production in individual bacteria.[123] These studies allow for the study of low copy number RNAs and proteins. This approach has also been expanded to study the binding of transcription factors in both prokaryotes and eukaryotes.[108,124,125]

Counting in vivo has been taken even farther to measure the dynamics of complicated molecular machines as they replicate bacterial genomes.[126] This approach relies on acquiring data at a 3 ms rate and averaging the data into 90 ms windows.[127] This improved acquisition time makes the measurement less sensitive to the noise of fluorescence emission. Impressively, the broad distributions of photobleaching steps observed for multiple replisome components show a bimodal distribution, indicative of two replisomes in close proximity. This method was further implemented to study bacterial chromosome compaction by MukBEF proteins, looking at two colors simultaneously to examine complex stoichiometry, as well as combine with tracking to measure the diffusion of chromosomal components.[128]

Encyclopedia of Analytical Chemistry, Online © 2006–2015 John Wiley & Sons, Ltd.

This article was published in the *Encyclopedia of Analytical Chemistry* in 2015 by John Wiley & Sons, Ltd.
DOI: 10.1002/9780470027318.a9494

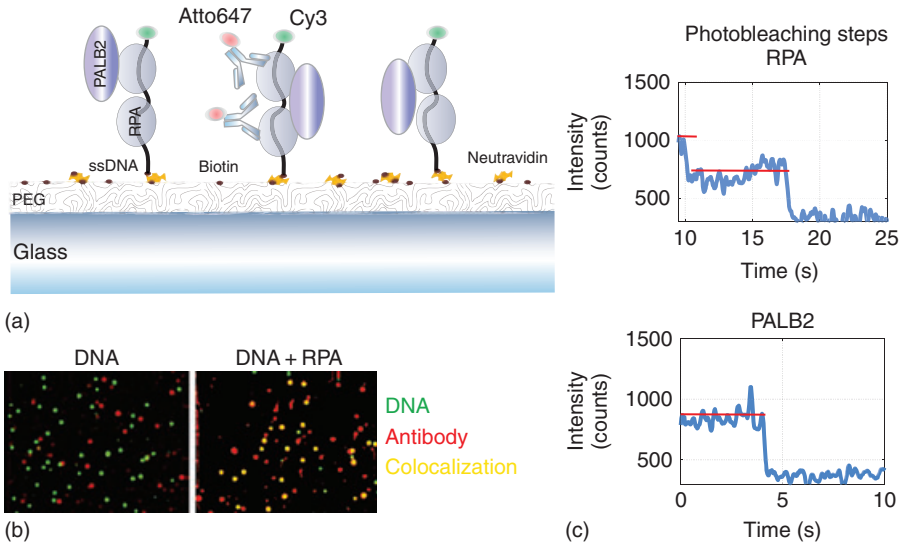

Figure 3 Single-molecule photobleaching. (a) Cartoon showing single-stranded DNA with Cy3 bound to biotin-PEG surface through neutravidin linked. Single-stranded DNA binding protein RPA is allowed to bind to the DNA, while PALB2 is free to bind RPA. The presence of PALB2 is then probed with fluorescently tagged antibodies. (b) Images from single-molecule pulldown experiments. A DNA-only control shows no colocalization with fluorescently labeled antibody. The addition of a nuclear extract with RPA and PALB2 shows increased colocalization. (c) Using antibodies to either PALB2 or fluorescently tagged-RPA, photobleaching steps are clearly seen.

7 SUPER-RESOLUTION MICROSCOPY

7.1 Single-molecule Fluorescence Localization Super-resolution Microscopy

The most recent conceptual advancements in light microscopy have improved image resolution up to 10-fold beyond the diffraction limit.[25] Super-resolution microscopy enables to study various cellular processes at the length scale much closer to that of individual proteins. The term super-resolution microscopy is attributed to three different imaging approaches: (i) fluorescent localization microscopy (FLM), (ii) stimulated emission depletion (STED) microscopy, and (iii) structured illumination microscopy (SIM).[11,129,130] While all three microscopy approaches offer imaging capabilities with subdiffraction resolution, SIM provides only twofold improvement in resolution (from 250 to 120 nm), whereas FLM and STED microscopy offer resolution well below 100 nm.[11,131,132] Of these methods, only FLM is based on single-molecule detection, which is the focus of this article. We also note that instruments for FLM methods are more affordable and require considerably less hardware and are easier to implement when compared to SIM and STED microscopy.[11]

FLM methods are essentially based on the principle of FIONA, where a diffraction-limited spot is localized with nanometer accuracy, with the excitation that instead of localization of only one spot, many spots are localized for imaging whole cells and tissue samples. The main feature of these techniques is the ability to localize individual fluorophores, which is necessary for nanoscale imaging, in a heavily labeled sample, as the specific cellular features need to be highly labeled to accurately reconstruct a super-resolved image. This is achieved through a stochastic on–off–on switching of subsets of fluorophores in the sample, utilizing unique photophysical properties of fluorophores. The on–off switching process is stochastic, so only a visually sparse subset of the fluorophores will emit in each frame. To reconstruct a super-resolved image, movies consisting of numerous switching cycles of a labeled biological sample are recorded. This is followed by analysis in which the spots in each frame are localized, and their resulting coordinates are plotted to give the super-resolved image. The first two pioneering FLM methods that demonstrated this approach are stochastic reconstruction microscopy (STORM), which uses coupled organic dyes (Cy3 and Cy5) and photoactivation localization microscopy (PALM), which uses fluorescent proteins that can be activated or induce spectral shift using light.[133,134]

Recently, simplified versions of these techniques were realized. These methods utilize fluorescence intermittency (or blinking) and photobleaching event of fluorophores to localize individual molecules and generate super-resolved images.[135,136] The blinking behavior is a stochastic process that arises from the recurring transition

Encyclopedia of Analytical Chemistry, Online © 2006–2015 John Wiley & Sons, Ltd.

This article was published in the *Encyclopedia of Analytical Chemistry* in 2015 by John Wiley & Sons, Ltd.
DOI: 10.1002/9780470027318.a9494

Table 1 A list of fluorescent proteins and dyes used in the most common super-resolution microscopy techniques

PALM fluorescent proteins	STORM Dyes[137]	dSTORM Dyes[138]
mEos[133]	ATTO 488	Alexa Fluor 488
mEos2[139]	Alexa Fluor 488	Dy 505
mEos3.2[139]	ATTO 520	Rhodamine 123
mCalvGR2[139]	Fluorescein	ATTO 488
mMaple[139]	FITC	SNAP-Cell 505
Dendra2[139]	Cy2	Rhodamine 6G
PA-GFP[139]	Cy3B	ATTO 520
PA-mCherry[140]	Alexa Fluor 568	Dy 530
Dronpa[141]	Cy3	ATTO 532
	Cy3.5	Alexa Fluor 532
	ATTO 565	SNAP-Cell TMR-Star
	Alexa Fluor 647	ATTO 565
	Cy5	Alexa Fluor 568
	ATTO 647	ATTO 590
	ATTO 647N	Alexa Fluor 647
	Dyomics 654	Cy5
	ATTO 655	ATTO 655
	ATTO 680	
	Cy5.5	ATTO 680
	DyLight 750	ATTO 700
	Cy7	Cy3
	Alexa Fluor 750	Alexa Fluor 700
	ATTO 740	Alexa Fluor 680
	Alexa Fluor 790	Alexa Fluor 750

of the emitter between a nonemitting state (off) and an emitting state (on). A table of the most prevalent PALM and STORM fluorophores is provided in Table 1.[137−141] The rate of transition and duration in each state depends on a number of parameters, such as irradiation intensity and buffer conditions (oxidizing agents, reducing agents, and free oxygen), and it can be tuned accordingly. The advantage of these methods is that only an excitation laser is needed, whereas photoactivation requires both activation and excitation lasers. There are different subsets of these methods that vary by the density of fluorophores in the sample, analysis algorithms used to reconstruct the super-resolved image, and whether or not considerable photobleaching is present. The most commonly used FLM-based method is direct stochastic reconstruction microscopy (dSTORM), but the application of other closely related FLM subtypes such as gSHRIMP, SOFI, and DAOSTORM is gradually increasing.[135,142−147]

In the past several years, FLM has found a role in the elucidation of large macromolecular and other cellular structures. It has been used to understand the scaffolding of nuclear pores by labeling the Nup107-160 subcomplex at various points.[148] By labeling each component of the symmetrical complex in series and creating particle averages, a full model for the structure was generated. Another key example of FLMs use in understanding macromolecular structure was its application to understand the domain organization of the centrosome. The centrosome organizes microtubules in cells and is surrounded by a pericentriolar material, which appears as a diffuse haze in electron microscopy.[149] These studies showed that the pericentriolar material is organized into two domains, one proximal to the centriole and proteins extending from this in a matrix, primarily organized by pericentrin-like protein.[149,150] Again, this type of study used particle averaging to generate a structural picture of the average centrosome.[149] Using FLM for this type of structural study complements electron microscopy and crystallography approaches. Furthermore, FLM has been employed to study fine structural elements to better understand the organization of the shelterin complex, which protects telomeres from degradation.[151] This study used FLM to complement molecular and cell biological approaches by knocking down the complex and assay the state of the t-loop for structural integrity.

In Figure 4(a), we show the principle of FLM, where stochastically emitting fluorophores are localized below the diffraction limit. New localization events are mapped as old fluorophores deactivate and new ones activate, allowed for a fully super-resolution image to be reconstructed. We provide an example of the enhanced imaging capabilities of FLM in Figure 4(b), comparing

Encyclopedia of Analytical Chemistry, Online © 2006–2015 John Wiley & Sons, Ltd.

This article was published in the *Encyclopedia of Analytical Chemistry* in 2015 by John Wiley & Sons, Ltd.
DOI: 10.1002/9780470027318.a9494

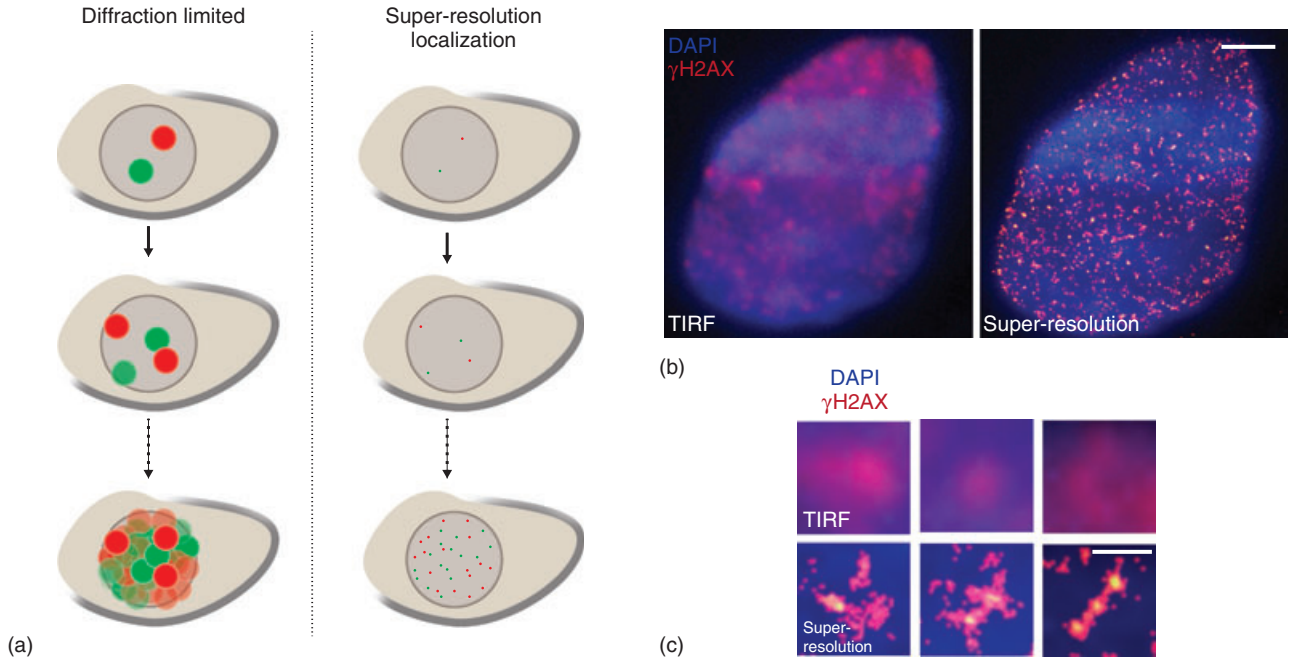

Figure 4 Super-resolution microscopy by localization. (a) Cartoon illustrating data acquisition in super-resolution microscopy achieved by fluorescence localization. Emission from a visually sparse set of dyes is collected, allowing for the precise fitting of each according to FIONA (resolution enhancement in the cartoon is to scale). As more points are collected, a super-resolved image is built from the accumulated points. (b) Nucleus of a cell stained for γH2AX. The TIRF image on the left is diffraction-limited resolution, whereas the super-resolved reconstruction on the right shows enhanced spatial features. Scale bar is 5 μm. (c) Selected zoom regions showing enhanced spatial features inaccessible by normal microscopy. Scale bar is 500 nm.

a regular fluorescence image and reconstructed super-resolved image of DNA stained with DAPI and immunofluorescently labeled DNA damage response marker, γH2AX.[152] In contrast to the diffraction-limited blurred γH2AX foci, the super-resolve foci show significantly enhanced spatial features.

7.2 3-D Super-resolution Microscopy

Super resolution along the *z*-axis has been achieved through two innovative methods. In the first approach, a cylindrical lens was introduced into the emission path to generate axial astigmatism as described earlier. This approach was applied for structural studies related to organelle organization in mammalian cells, imaging synapses, or visualizing the nanoscale organization of bacterial *Z*-rings, the site of bacterial cell division.[153−156] The second approach uses interferometry of the emitted photons collected along two different paths to determine 3-D positioning information.[157] This approach requires more technical complexity but provides significant improvement in *z*-position accuracy. Presently, this approach has only been applied to the visualization of basic cellular structures such as microtubules, plasma membrane, and integrin receptors.[157,158] Finally, it should be noted that 3-D imaging can also be performed with quantum dots, which are novel semiconductor-based nanostructure that provide improved fluorescence emission and stability as compared to fluorescent dyes and proteins.[159]

7.3 Imaging Buffer for Proper Fluorescent Localization Microscopy

Numerous approaches have been employed to improve the number of photons collected to increase the resolution of super-resolution reconstructions. It is also important to consider the time frame required to collect sufficient data for a reconstruction. The simplest improvements are to add compounds to the imaging buffers in STORM- and dSTORM-based techniques. Oxygen-scavenging systems mentioned earlier such as PCA/PCD and glucose oxidase (Gloxy) enhance dye photostability. In addition, compounds such as cyclooctatetraene (COT) and deuterated water can be added to improve the output of photons.[160,161] Additional changes in instrumentation, such as stronger lasers for imaging, or collecting light with two objective lenses can improve the number of photons emitted and collected.[162] With the best localization of a single dye reported at subnanometer accuracy,

Encyclopedia of Analytical Chemistry, Online © 2006–2015 John Wiley & Sons, Ltd.

This article was published in the *Encyclopedia of Analytical Chemistry* in 2015 by John Wiley & Sons, Ltd.
DOI: 10.1002/9780470027318.a9494

there exist some reasonable improvements to present super-resolution techniques, allowing for more nuanced structural features to be captured by this approach.[163]

7.4 Analysis of Super-resolution Imaging

Numerous freeware programs now exist that allow for the simple and fast reconstruction of FLM data sets. Some examples are QuickPALM 3D, RapidSTORM, plam3d, and ThunderSTORM.[164−167] Nevertheless, the generation of super-resolved images presents new challenges for analysis. The enhanced detection efficiency and nanoscale imaging capabilities of FLM result in abundance of previously unattainable data, providing the precise dimensions, shape, next neighbor proximity, cellular density, and connectivity of specific molecules and molecular clusters.[168] For instance, objects perceived in diffraction-limited microscopy as 'diffused' background now form detailed shapes as specific molecular clusters; further, while the overlap of two-color objects in confocal images is estimated using correlation functions (such as Pearson coefficients), in super-resolution data, the specific area of overlap can be directly extracted.[169] The utilization of super-resolution microscopy in biomedical research involves more than development and validations – it requires new standardized tools for big-data analysis, robust statistics, and modeling. Deriving quantifiable and meaningful data from the obtained super-resolution images requires the development of new computational tools to enable proper extraction, sorting, and automation of big-data image analysis.[144,151,170−174]

8 CURRENT APPLICATIONS OF SINGLE-MOLECULE TECHNIQUES

8.1 DNA Sequencing by Single-molecule Fluorescence

An important application of single-molecule fluorescence has been in the field of DNA sequencing technology. DNA sequencing presents several unique challenges, requiring good sequence read fidelity and sequence read length.[175] The sequence read fidelity is the quality of the signal for each nucleotide incorporated on a template strand providing the readout. The read length is how many nucleotides can be read in each sequencing reaction. Measuring the incorporation of nucleotides using single-molecule fluorescence has been beneficial in that the quality of each DNA read enjoys excellent S/N and long read lengths owing to the specific DNA polymerase used. DNA polymerases vary in their enzymatic processivity, with read lengths varying based on structural factors.[176] The typical polymerase chosen for single-molecule sequencing is Φ29 DNA polymerase, which has a build in sliding clamp, which raises processivity to the order of ∼5 kbs.[175]

The issue of measuring fluorescently incorporated nucleotides has been solved through clever materials engineering. Typically, TIRF microscopes lose their ability to distinguish molecules near the surface when the concentration of fluorescently labeled molecules approaches 20 nm.[177] In order to measure incorporation of fluorescent nucleotides with reasonable S/N, single-molecule DNA sequencing makes use of a zero-mode waveguide. A zero-mode waveguide is a nanostructure where holes on the order of 20 nm have been etched in an array pattern.[177,178] This structure is anchored a passivized coverslip, forming small pores near the surface and a large flow cells behind the array. Owing to their small size, epifluorescent excitation results in an evanescent wave front in each of these small zeptoliter-sized pores. The small volume and this excitation scheme allow for a much higher solution concentration of labeled nucleotides for sequencing. Each nucleotide is labeled on the terminal phosphate with a spectrally distinct dye, when the polymerase incorporating nucleotides cleaves the pyrophosphate from the nucleotide; the fluorescence signal is free to diffuse away.[175]

In this instrument, all fluorescence emission is collected from these diffraction-limited pores and sheered with a prism.[179] With the four nucleotides, each is labeled at different color, so that each color will be registered by a separate pixel on an EMCCD detector.[179] In this manner, hundreds of long DNA reads can be generated simultaneously from the same acquisition. This essentially allows for counting molecules as they interact with biological molecules, which gives measurement kinetics over long timescales. This technology has been recently expanded to include the study of protein synthesis by ribosomes.[180] It is likely that this attractive approach will expand to measure the stoichiometry and kinetics of complex biological systems.

9 CONCLUSIONS

Single-molecule fluorescence microscopy methods are still quite technically challenging to utilize but provide important new data that cannot be obtained with any other means, offering a deeper understanding of the underlying principles guiding biology. The future will see an increasing demand for this technology and related expertise, and the development of new commercial applications of these methods.[181] The desire to extract more meaningful information from biological samples will lead to the combinations of approaches, with tracking, smFRET, stoichiometry, and super resolution all likely occurring simultaneously.[182] Super resolution is also

Encyclopedia of Analytical Chemistry, Online © 2006–2015 John Wiley & Sons, Ltd.

This article was published in the *Encyclopedia of Analytical Chemistry* in 2015 by John Wiley & Sons, Ltd.
DOI: 10.1002/9780470027318.a9494

being slowly combined with electron microscopy imaging to further understand the biological ultrastructure.[183,184] In vitro single-molecule fluorescence experiments will likely follow a similar trend, relying more on pulling down cellular materials for study, identifying stoichiometry, and selectively probing interactions. We also anticipate that as the technology comes of age, high-throughput methods will expand the field into new areas such as drug discovery and medical diagnostics.[185–187]

ABBREVIATIONS AND ACRONYMS

DIY	Do-It-Yourself
NA	Numerical Aperture
PMT	Photomultiplier Tube
APD	Avalanche Photo Diode
QE-CCD	Quantum Efficiency Charge Couple Device
CCD	Charge Couple Device
ICCD	Intensified Charge Couple Device
EMCCD	Electron Multiplying Charge Couple Device
sCMOS	Scientific Complementary Metal-Oxide Semiconductor
S/N	Signal-to-Noise Ratio
TIRF	Total Internal Reflection Fluorescence
TIR	Total Internal Reflection
FRET	Forster Resonance Energy Transfer
smFRET	single-molecule Fluorescence Resonance Energy Transfer
BSA	Bovine Serum Albumin
PEG	Polyethylene Glycol
PCA	Protocatechuate Acid
PCD	Protocatechuate-3,4-Dioxygenase
FP	Fluorescence Polarization
FA	Fluorescence Anisotropy
ATP	Adenosine Triphosphate
ADP	Adenosine Diphosphate
PSF	Point Spread Function
NSOM	Near-Field Scanning Optical Microscopy
FIONA	Fluorescence Imaging with One Nanometer Accuracy
RPA	Replication Protein A
FLM	Fluorescent Localization Microscopy
STED	Stimulated Emission Depletion
SIM	Structured Illumination Microscopy
STORM	Stochastic Reconstruction Microscopy
PALM	Photoactivation Localization Microscopy
dSTORM	direct Stochastic Reconstruction Microscopy
COT	Cyclooctatetraene

RELATED ARTICLES

Biomedical Spectroscopy **(Volume 1)**
Biomedical Spectroscopy: Introduction

Biomedical Spectroscopy **(Volume 1)**
Fluorescence Imaging

Biomedical Spectroscopy **(Volume 1)**
Fluorescence Spectroscopy In Vivo

Biomolecules Analysis **(Volume 1)**
Biomolecules Analysis: Introduction

Biomolecules Analysis **(Volume 1)**
Fluorescence-based Biosensors

Biomolecules Analysis **(Volume 1)**
Single Biomolecule Detection and Characterization

Clinical Chemistry **(Volume 2)**
Immunochemistry

Nucleic Acids Structure and Mapping **(Volume 6)**
DNA Molecules, Properties and Detection of Single

REFERENCES

1. B.N. Giepmans, S.R. Adams, M.H. Ellisman, R.Y. Tsien, 'The Fluorescent Toolbox for Assessing Protein Location and Function', *Science*, **312**, 217–224 (2006). DOI: 10.1126/science.1124618
2. A.H. Coons, 'The Beginnings of Immunofluorescence', *J. Immunol.*, **87**, 499–503 (1961).
3. M. Yanagida, Y. Hiraoka, I. Katsura, 'Dynamic Behaviors of DNA Molecules in Solution Studied by Fluorescence Microscopy', *Cold Spring Harb. Symp. Quant. Biol.*, **47**(Pt 1), 177–187 (1983).
4. S.B. Smith, P.K. Aldridge, J.B. Callis, 'Observation of Individual DNA Molecules Undergoing gel Electrophoresis', *Science*, **243**, 203–206 (1989).
5. P. Qin, D. Yu, X. Zuo, P.V. Cornish, 'Structured mRNA Induces the Ribosome into a Hyper-Rotated State', *EMBO Rep.*, **15**, 185–190 (2014). DOI: 10.1002/embr.201337762
6. H. Noji, R. Yasuda, M. Yoshida, K. Kinosita Jr, 'Direct Observation of the Rotation of F1-ATPase', *Nature*, **386**, 299–302 (1997). DOI: 10.1038/386299a0
7. K. Adachi, K. Oiwa, T. Nishiz aka, *et al.*, 'Coupling of Rotation and Catalysis in F(1)-ATPase Revealed by Single-Molecule Imaging and Manipulation', *Cell*, **130**, 309–321 (2007). DOI: 10.1016/j.cell.2007.05.020

Encyclopedia of Analytical Chemistry, Online © 2006–2015 John Wiley & Sons, Ltd.

This article was published in the *Encyclopedia of Analytical Chemistry* in 2015 by John Wiley & Sons, Ltd.
DOI: 10.1002/9780470027318.a9494

8. S.H. Sternberg, S. Redding, M. Jinek, E.C. Greene, J.A. Doudna, 'DNA Interrogation by the CRISPR RNA-Guided Endonuclease Cas9', *Nature*, **507**, 62–67 (2014). DOI: 10.1038/nature13011
9. M. Greenfeld, D.S. Pavlichin, H. Mabuchi, D. Herschlag, 'Single Molecule Analysis Research Tool (SMART): an Integrated Approach for Analyzing Single Molecule Data', *PLoS One*, **7**, e30024 (2012). DOI: 10.1371/journal.pone.0030024
10. T. Holm, T. Klein, A. Löschberger, *et al.*, 'A Blueprint for Cost-Efficient Localization Microscopy', *Chemphyschem: Eur. J. Chem. Phys. Phys. Chem.*, **15**, 651–654 (2014). DOI: 10.1002/cphc.201300739
11. B. Huang, M. Bates, X. Zhuang, 'Super-Resolution Fluorescence Microscopy', *Annu. Rev. Biochem.*, **78**, 993–1016 (2009). DOI: 10.1146/annurev.biochem.77.061906.092014
12. B. Huang, H. Babcock, X. Zhuang, 'Breaking the Diffraction Barrier: Super-Resolution Imaging of Cells', *Cell*, **143**, 1047–1058 (2010). DOI: 10.1016/j.cell.2010.12.002
13. E. Rothenberg, T. Ha, 'Single-Molecule FRET Analysis of Helicase Functions', *Methods in molecular biology*, **587**, 29–43 (2010). DOI: 10.1007/978-1-60327-355-8_3
14. P.R. Selvin, T. Ha, *Single-molecule techniques: a laboratory manual*, Cold Spring Harbor Laboratory Press, Cold Spring Harbor, NY, 2008.
15. P. Hinterdorfer, A. Van Oijen, *Handbook of Single-molecule Biophysics*, Springer, Berlin, 2009.
16. D.B. Murphy, M.W. Davidson, Fundamentals of Light Microscopy and Electronic Imaging, 2nd edition, Wiley-Blackwell, Hoboken, NJ, 2013.
17. Y. Hiraoka, J.W. Sedat, D.A. Agard, 'The use of a Charge-Coupled Device for Quantitative Optical Microscopy of Biological Structures', *Science*, **238**, 36–41 (1987).
18. W. Zhang, Y. Jiang, Q. Wang, *et al.*, 'Single-Molecule Imaging Reveals Transforming Growth Factor-Beta-Induced Type II Receptor Dimerization', *Proc. Natl. Acad. Sci. U. S. A.*, **106**, 15679–15683 (2009). DOI: 10.1073/pnas.0908279106
19. X. Michalet, O.H.W. Siegmund, J.V. Vallerga, *et al.*, 'Detectors for Single-molecule Fluorescence Imaging and Spectroscopy', *J. Mod. Opt.*, **54**, 239 (2007). DOI: 10.1080/09500340600769067
20. X.H. Fang, W.H. Tan, 'Imaging Single Fluorescent Molecules at the Interface of an Optical Fiber Probe by Evanescent Wave Excitation', *Anal. Chem.*, **71**, 3101–3105 (1999). DOI: 10.1021/Ac990225w
21. X. Michalet, R.A. Colyer, G. Scalia, *et al.*, 'Development of New Photon-counting Detectors for Single-molecule Fluorescence Microscopy', *Philos. Trans. R. Soc. Lond. B Biol. Sci.*, **368**, 20120035 (2013). DOI: 10.1098/rstb.2012.0035
22. F. Huang, T.M. Hartwich, F.E. Rivera-Molina, *et al.*, 'Video-Rate Nanoscopy Using sCMOS Camera-Specific Single-Molecule Localization Algorithms', *Nat. Methods*, **10**, 653–658 (2013). DOI: 10.1038/nmeth.2488
23. H.T. Beier, B.L. Ibey, 'Experimental Comparison of the High-Speed Imaging Performance of an EM-CCD and sCMOS Camera in a Dynamic Live-Cell Imaging Test Case', *PLoS One*, **9**, e84614 (2014). DOI: 10.1371/journal.pone.0084614
24. H. Ma, H. Kawai, E. Toda, S. Zeng, Z.L. Huang, 'Localization-based Super-resolution Microscopy with an sCMOS Camera Part III: Camera Embedded Data Processing Significantly Reduces the Challenges of Massive Data Handling', *Opt. Lett.*, **38**, 1769–1771 (2013). DOI: 10.1364/OL.38.001769
25. D. Toomre, J. Bewersdorf, 'A New Wave of Cellular Imaging', *Annu. Rev. Cell Dev. Biol.*, **26**, 285–314 (2010). DOI: 10.1146/annurev-cellbio-100109-104048
26. M.L. Martin-Fernandez, C.J. Tynan, S.E. Webb, 'A Pocket Guide' to Total Internal Reflection Fluorescence', *J. Microsc.*, **252**, 16–22 (2013). DOI: 10.1111/jmi.12070
27. S.J. Holden, S. Uphoff, J. Hohlbein, *et al.*, 'Defining the Limits of Single-molecule FRET Resolution in TIRF Microscopy', *Biophys. J.*, **99**, 3102–3111 (2010). DOI: 10.1016/j.bpj.2010.09.005
28. L. Groc, M. Heine, S.L. Cousins, *et al.*, 'NMDA Receptor Surface Mobility Depends on NR2A-2B Subunits', *Proc. Natl. Acad. Sci. U. S. A.*, **103**, 18769–18774 (2006). DOI: 10.1073/pnas.0605238103
29. C. Bats, L. Groc, D. Choquet, 'The Interaction between Stargazin and PSD-95 Regulates AMPA Receptor Surface Trafficking', *Neuron*, **53**, 719–734 (2007). DOI: 10.1016/j.neuron.2007.01.030
30. L. Bard, M. Sainlos, D. Bouchet, *et al.*, 'Dynamic and Specific Interaction Between Synaptic NR2-NMDA Receptor and PDZ Proteins', *Proc. Natl. Acad. Sci. U. S. A.*, **107**, 19561–19566 (2010). DOI: 10.1073/pnas.1002690107
31. P. Opazo, S. Labrecque, C.M. Tigaret, *et al.*, 'CaMKII Triggers the Diffusional Trapping of Surface AMPARs Through Phosphorylation of Stargazin', *Neuron*, **67**, 239–252 (2010). DOI: 10.1016/j.neuron.2010.06.007
32. P.E. Hanninen, S.W. Hell, J. Salo, E. Soini, C. Cremer, '2-Photon Excitation 4pi Confocal Microscope – Enhanced Axial Resolution Microscope for Biological-Research', *Appl. Phys. Lett.*, **66**, 1698–1700 (1995).
33. S.W. Hell, P.E. Hanninen, M. Schrader, T. Wilson, E. Soini, 'Resolution Beyond the Diffraction Limit - 4pi-Confocal, STED, and GSD', *Zool. Stud.*, **34**, 70 (1995).
34. S.L. Reck-Peterson, N.D. Derr, N. Stuurman, 'Imaging Single Molecules Using Total Internal Reflection Fluorescence Microscopy (TIRFM)', *Cold Spring Harb. Protoc.*, **2010**(3), pdb top73 (2010). DOI: 10.1101/pdb.top73
35. J.G. Ritter, R. Veith, A. Veenendaal, J.P. Siebrasse, U. Kubitscheck, 'Light sheet Microscopy for Single

Encyclopedia of Analytical Chemistry, Online © 2006–2015 John Wiley & Sons, Ltd.

This article was published in the *Encyclopedia of Analytical Chemistry* in 2015 by John Wiley & Sons, Ltd.
DOI: 10.1002/9780470027318.a9494

Molecule Tracking in Living Tissue', *PLoS One*, **5**, e11639 (2010). DOI: 10.1371/journal.pone.0011639

36. Y. Li, Y. Hu, H. Cang, 'Light Sheet Microscopy for Tracking Single Molecules on the Apical Surface of Living Cells', *J. Phys. Chem. B*, **117**, 15503–15511 (2013). DOI: 10.1021/jp405380g
37. M. Tokunaga, N. Imamoto, K. Sakata-Sogawa, 'Highly Inclined Thin Illumination Enables Clear Single-molecule Imaging in Cells', *Nat. Methods*, **5**, 159–161 (2008). DOI: 10.1038/nmeth1171
38. R. Roy, S. Hohng, T. Ha, 'A Practical Guide to Single-molecule FRET', *Nat. Methods*, **5**, 507–516 (2008). DOI: 10.1038/nmeth.1208
39. J.R. Lakowicz, *Principles of Fluorescence Spectroscopy*, 3rd edition, Springer, Berlin, 2006.
40. C. Joo, H. Balci, Y. Ishitsuka, C. Buranachai, T. Ha, 'Advances in Single-molecule Fluorescence Methods for Molecular Biology', *Annu. Rev. Biochem.*, **77**, 51–76 (2008). DOI: 10.1146/annurev.biochem.77.070606.101543
41. L. Stryer, R.P. Haugland, 'Energy Transfer: a Spectroscopic Ruler', *Proc. Natl. Acad. Sci. U. S. A.*, **58**, 719–726 (1967).
42. S.A. McKinney, A.C. Declais, D.M. Lilley, T. Ha, 'Structural Dynamics of Individual Holliday Junctions', *Nat. Struct. Biol.*, **10**, 93–97 (2003). DOI: 10.1038/nsb883
43. I. Rasnik, S. Myong, W. Cheng, T.M. Lohman, T. Ha, 'DNA-binding Orientation and Domain Conformation of the E. coli rep Helicase Monomer Bound to a Partial Duplex Junction: Single-Molecule Studies of Fluorescently Labeled Enzymes', *J. Mol. Biol.*, **336**, 395–408 (2004).
44. S. Myong, M.M. Bruno, A.M. Pyle, T. Ha, 'Spring-loaded Mechanism of DNA Unwinding by Hepatitis C Virus NS3 Helicase', *Science*, **317**, 513–516 (2007). DOI: 10.1126/science.1144130
45. T. Ha, T. Enderle, S. Chemla, R. Selvin, S. Weiss, 'Single Molecule Dynamics Studied by Polarization Modulation', *Phys. Rev. Lett.*, **77**, 3979–3982 (1996).
46. E. Tan, T.J. Wilson, M.K. Nahas, *et al.*, 'A Four-way Junction Accelerates Hairpin Ribozyme Folding Via a Discrete Intermediate', *Proc. Natl. Acad. Sci. U. S. A.*, **100**, 9308–9313 (2003). DOI: 10.1073/pnas.1233536100
47. T. Ha, I. Rasnik, W. Cheng, *et al.*, 'Initiation and Re-initiation of DNA Unwinding by the Escherichia coli Rep Helicase', *Nature*, **419**, 638–641 (2002). DOI: 10.1038/nature01083
48. F. Persson, J. Fritzsche, J.O. Tegenfeldt, *et al.*, 'Lipid-based Passivation in Nanofluidics', *Nano Lett.*, **12**, 2260–2265 (2012). DOI: 10.1021/nl204535h
49. I. Cisse, B. Okumus, C. Joo, T. Ha, 'Fueling Protein DNA Interactions Inside Porous Nanocontainers', *Proc. Natl. Acad. Sci. U. S. A.*, **104**, 12646–12650 (2007). DOI: 10.1073/pnas.0610673104
50. I.I. Cisse, H. Kim, T. Ha, 'A rule of Seven in Watson-Crick Base-pairing of Mismatched Sequences', *Nat. Struct. Mol. Biol.*, **19**, 623–627 (2012). DOI: 10.1038/nsmb.2294
51. B.J. Frisken, C. Asman, P.J. Patty, 'Studies of Vesicle Extrusion', *Langmuir*, **16**, 928–933 (2000). DOI: 10.1021/La9905113
52. M.E. Bowen, K. Weninger, A.T. Brunger, S. Chu, 'Single Molecule Observation of Liposome-bilayer Fusion Thermally Induced by Soluble N-ethyl Maleimide Sensitive-factor Attachment Protein Receptors (SNAREs)', *Biophys. J.*, **87**, 3569–3584 (2004). DOI: 10.1529/biophysj.104.048637
53. Z. Su, Y. Ishitsuka, T. Ha, Y.K. Shin, 'The SNARE Complex From Yeast is Partially Unstructured on the Membrane', *Structure*, **16**, 1138–1146 (2008). DOI: 10.1016/j.str.2008.03.018
54. T.Y. Yoon, B. Okumus, F. Zhang, Y.K. Shin, T. Ha, 'Multiple Intermediates in SNARE-induced Membrane Fusion', *Proc. Natl. Acad. Sci. U. S. A.*, **103**, 19731–19736 (2006). DOI: 10.1073/pnas.0606032103
55. Y. Wang, Y. Liu, H.A. Deberg, *et al.*, 'Single Molecule FRET Reveals Pore Size and Opening Mechanism of a Mechano-sensitive Ion Channel', *eLife*, **3**, e01834 (2014). DOI: 10.7554/eLife.01834
56. A.N. Kapanidis, N.K. Lee, T.A. Laurence, *et al.*, 'Fluorescence-aided Molecule Sorting: Analysis of Structure and Interactions by Alternating-laser Excitation of Single Molecules', *Proc. Natl. Acad. Sci. U. S. A.*, **101**, 8936–8941 (2004). DOI: 10.1073/pnas.0401690101
57. A.N. Kapanidis, T.A. Laurence, N.K. Lee, *et al.*, 'Alternating-laser Excitation of Single Molecules', *Acc. Chem. Res.*, **38**, 523–533 (2005). DOI: 10.1021/ar0401348
58. N.K. Lee, A.N. Kapanidis, H.R. Koh, *et al.*, 'Three-color Alternating-laser Excitation of Single Molecules: Monitoring Multiple Interactions and Distances', *Biophys. J.*, **92**, 303–312 (2007). DOI: 10.1529/biophysj.106.093211
59. M.F. Garcia-Parajo, J.A. Veerman, R. Bouwhuis, R. Vallee, N.F. van Hulst, 'Optical Probing of Single Fluorescent Molecules and Proteins', *Chemphyschem: Eur. J. Chem. Phys. Phys. Chem.*, **2**, 347–360 (2001). DOI: 10.1002/1439-7641(20010618)2:6<347::AID-CPHC347>3.0.CO;2–7
60. C.E. Aitken, R.A. Marshall, J.D. Puglisi, 'An Oxygen Scavenging System for Improvement of Dye Stability in Single-molecule Fluorescence Experiments', *Biophys. J.*, **94**, 1826–1835 (2008). DOI: 10.1529/biophysj.107.117689
61. I. Rasnik, S.A. McKinney, T. Ha, 'Nonblinking and Long-lasting Single-molecule Fluorescence Imaging', *Nat. Methods*, **3**, 891–893 (2006). DOI: 10.1038/nmeth934
62. E. Rothenberg, J.M. Grimme, M. Spies, T. Ha, 'Human Rad52-Mediated Homology Search and Annealing Occurs by Continuous Interactions Between Overlapping

Encyclopedia of Analytical Chemistry, Online © 2006–2015 John Wiley & Sons, Ltd.

This article was published in the *Encyclopedia of Analytical Chemistry* in 2015 by John Wiley & Sons, Ltd.
DOI: 10.1002/9780470027318.a9494

Nucleoprotein Complexes', *Proc. Natl. Acad. Sci. U. S. A.*, **105**, 20274–20279 (2008). DOI: 10.1073/pnas.0810317106

63. E. Rothenberg, M.A. Trakselis, S.D. Bell, T. Ha, 'MCM Forked Substrate Specificity Involves Dynamic Interaction With the 5'-tail', *J. Biol. Chem.*, **282**, 34229–34234 (2007). DOI: 10.1074/jbc.M706300200
64. S. Myong, I. Rasnik, C. Joo, T.M. Lohman, T. Ha, 'Repetitive Shuttling of a Motor Protein on DNA', *Nature*, **437**, 1321–1325 (2005). DOI: 10.1038/nature04049
65. S.A. McKinney, C. Joo, T. Ha, 'Analysis of Single-molecule FRET Trajectories Using Hidden Markov Modeling', *Biophys. J.*, **91**, 1941–1951 (2006). DOI: 10.1529/biophysj.106.082487
66. D.L. Floyd, S.C. Harrison, A.M. van Oijen, 'Analysis of Kinetic Intermediates in Single-Particle Dwell-time Distributions', *Biophys. J.*, **99**, 360–366 (2010). DOI: 10.1016/j.bpj.2010.04.049
67. S. Syed, M. Pandey, S.S. Patel, T. Ha, 'Single-molecule Fluorescence Reveals the Unwinding Stepping Mechanism of Replicative Helicase', *Cell Rep.*, **6**, 1037–1045 (2014). DOI: 10.1016/j.celrep.2014.02.022
68. T. Aggarwal, D. Materassi, R. Davison, T. Hays, M. Salapaka, 'Detection of Steps in Single Molecule Data', *Cell. Mol. Bioeng.*, **5**, 14–31 (2012). DOI: 10.1007/s12195-011-0188-5
69. B.C. Carter, M. Vershinin, S.P. Gross, 'A Comparison of Step-detection Methods: How Well Can You Do?', *Biophys. J.*, **94**, 306–319 (2008). DOI: 10.1529/biophysj.107.110601
70. J.W. van de Meent, J.E. Bronson, C.H. Wiggins, R.L. Gonzalez Jr, 'Empirical Bayes Methods Enable Advanced Population-level Analyses of Single-Molecule FRET Experiments', *Biophys. J.*, **106**, 1327–1337 (2014). DOI: 10.1016/j.bpj.2013.12.055
71. J.N. Forkey, M.E. Quinlan, Y.E. Goldman, 'Protein Structural Dynamics by Single-molecule Fluorescence Polarization', *Prog. Biophys. Mol. Biol.*, **74**, 1–35 (2000).
72. N. Hafi, M. Grunwald, L.S. van den Heuvel, *et al.*, 'Fluorescence Nanoscopy by Polarization Modulation and Polarization Angle Narrowing', *Nat. Methods*, **11**, 579–584 (2014). DOI: 10.1038/nmeth.2919
73. M.S. Nasir, M.E. Jolley, 'Fluorescence Polarization: an Analytical Tool for Immunoassay and Drug Discovery', *Comb. Chem. High Throughput Screen.*, **2**, 177–190 (1999).
74. W.A. Lea, A. Simeonov, 'Fluorescence Polarization Assays in Small Molecule Screening', *Expert Opin. Drug Discovery*, **6**, 17–32 (2011). DOI: 10.1517/17460441.2011.537322
75. H. Szmacinski, J.R. Lakowicz, 'Depolarization of Surface-enhanced Fluorescence: an Approach to Fluorescence Polarization Assays', *Anal. Chem.*, **80**, 6260–6266 (2008). DOI: 10.1021/ac8003055
76. C. Bustamante, D. Keller, G. Oster, 'The Physics of Molecular Motors', *Acc. Chem. Res.*, **34**, 412–420 (2001).
77. D. Keller, C. Bustamante, 'The Mechanochemistry of Molecular Motors', *Biophys. J.*, **78**, 541–556 (2000). DOI: 10.1016/S0006-3495(00)76615-X
78. J.N. Forkey, M.E. Quinlan, M.A. Shaw, J.E. Corrie, Y.E. Goldman, 'Three-dimensional Structural Dynamics of Myosin V by Single-Molecule Fluorescence Polarization', *Nature*, **422**, 399–404 (2003). DOI: 10.1038/nature01529
79. M.E. Quinlan, J.N. Forkey, Y.E. Goldman, 'Orientation of the Myosin Light Chain Region by Single Molecule Total Internal Reflection Fluorescence Polarization Microscopy', *Biophys. J.*, **89**, 1132–1142 (2005). DOI: 10.1529/biophysj.104.053496
80. S. Syed, G.E. Snyder, C. Franzini-Armstrong, P.R. Selvin, Y.E. Goldman, 'Adaptability of Myosin V Studied by Simultaneous Detection of Position and Orientation', *EMBO J.*, **25**, 1795–1803 (2006). DOI: 10.1038/sj.emboj.7601060
81. E. Toprak, J. Enderlein, S. Syed, *et al.*, 'Defocused Orientation and Position Imaging (DOPI) of Myosin V', *Proc. Natl. Acad. Sci. U. S. A.*, **103**, 6495–6499 (2006). DOI: 10.1073/pnas.0507134103
82. K. Adachi, R. Yasuda, H. Noji, *et al.*, 'Stepping Rotation of F1-ATPase Visualized Through Angle-resolved Single-fluorophore Imaging', *Proc. Natl. Acad. Sci. U. S. A.*, **97**, 7243–7247 (2000). DOI: 10.1073/pnas.120174297
83. K. Adachi, K. Oiwa, M. Yoshida, T. Nishizaka, K. Kinosita Jr, 'Controlled Rotation of the F(1)-ATPase Reveals Differential and Continuous Binding Changes for ATP Synthesis', *Nat. Commun.*, **3**, 1022 (2012). DOI: 10.1038/ncomms2026
84. T.J. Gould, M.S. Gunewardene, M.V. Gudheiti, *et al.*, 'Nanoscale Imaging of Molecular Positions and Anisotropies', *Nat. Methods*, **5**, 1027–1030 (2008). DOI: 10.1038/nmeth.1271
85. E. Abbe, 'Beiträge zur Theorie des Mikroskops und der Mikroskopischen Wahrnehmung', *Arch. Mikrosk. Anat.*, **9**, 413–418 (1873).
86. E. Betzig, A. Lewis, A. Harootunian, M. Isaacson, E. Kratschmer, 'Near Field Scanning Optical Microscopy (NSOM): Development and Biophysical Applications', *Biophys. J.*, **49**, 269–279 (1986).
87. U. Durig, D.W. Pohl, F. Rohner, 'Near-Field Optical-Scanning Microscopy', *J. Appl. Phys.*, **59**, 3318–3327 (1986).
88. J.R. Hahn, W. Ho, 'Single Molecule Imaging and Vibrational Spectroscopy with a Chemically Modified tip of a Scanning Tunneling Microscope', *Phys. Rev. Lett.*, **87**, 196102 (2001).
89. J.B. Decombe, J.F. Bryche, J.F. Motte, *et al.*, 'Transmission and Reflection Characteristics of Metal-coated Optical

Encyclopedia of Analytical Chemistry, Online © 2006–2015 John Wiley & Sons, Ltd.

This article was published in the *Encyclopedia of Analytical Chemistry* in 2015 by John Wiley & Sons, Ltd.
DOI: 10.1002/9780470027318.a9494

Fiber Tip Pairs', *Appl. Optics*, **52**, 6620–6625 (2013). DOI: 10.1364/Ao.52.006620

90. A. Yildiz, M. Tomishige, R.D. Vale, P.R. Selvin, 'Kinesin Walks Hand-over-hand', *Science*, **303**, 676–678 (2004). DOI: 10.1126/science.1093753
91. E. Toprak, H. Balci, B.H. Blehm, P.R. Selvin, 'Three-dimensional Particle Tracking Via Bifocal Imaging', *Nano Lett.*, **7**, 2043–2045 (2007). DOI: 10.1021/nl0709120
92. B. Huang, W. Wang, M. Bates, X. Zhuang, 'Three-dimensional Super-resolution Imaging by Stochastic Optical Reconstruction Microscopy', *Science*, **319**, 810–813 (2008). DOI: 10.1126/science.1153529
93. L. Holtzer, T. Meckel, T. Schmidt, 'Nanometric Three-dimensional Tracking of Individual Quantum Dots in Cells', *Appl. Phys. Lett.*, **90**, 053902 (2007). DOI: Artn 053902Doi 10.1063/1.2437066
94. I. Golding, E.C. Cox, 'RNA Dynamics in Live Escherichia Coli Cells', *Proc. Natl. Acad. Sci. U. S. A.*, **101**, 11310–11315 (2004). DOI: 10.1073/pnas.0404443101
95. I. Golding, J. Paulsson, S.M. Zawilski, E.C. Cox, 'Real-time Kinetics of Gene Activity in Individual Bacteria', *Cell*, **123**, 1025–1036 (2005). DOI: 10.1016/j.cell.2005.09.031
96. I. Golding, E.C. Cox, 'Physical Nature of Bacterial Cytoplasm', *Phys. Rev. Lett.*, **96**, 098102 (2006).
97. E. Rothenberg, L.A. Sepúlveda, S.O. Skinner, *et al.*, 'Single-virus Tracking Reveals a Spatial Receptor-dependent Search Mechanism', *Biophys. J.*, **100**, 2875–2882 (2011). DOI: 10.1016/j.bpj.2011.05.014
98. A. Yildiz, J.N. Forkey, S.A. McKineey, *et al.*, 'Myosin V Walks Hand-over-hand: Single Fluorophore Imaging With 1.5-nm Localization', *Science*, **300**, 2061–2065 (2003). DOI: 10.1126/science.1084398
99. A. Yildiz, M. Tomishige, A. Gennerich, R.D. Vale, 'Intramolecular Strain Coordinates Kinesin Stepping Behavior Along Microtubules', *Cell*, **134**, 1030–1041 (2008). DOI: 10.1016/j.cell.2008.07.018
100. C. Kural, H. Kim, S. Sued, *et al.*, 'Kinesin and Dynein Move a Peroxisome in Vivo: a Tug-of-war or Coordinated Movement?', *Science*, **308**, 1469–1472 (2005). DOI: 10.1126/science.1108408
101. C. Kural, A.S. Serpinskaya, Y.-H. Chou, *et al.*, 'Tracking Melanosomes Inside a Cell to Study Molecular Motors and Their Interaction', *Proc. Natl. Acad. Sci. U. S. A.*, **104**, 5378–5382 (2007). DOI: 10.1073/pnas.0700145104
102. M.A. DeWitt, A.Y. Chang, P.A. Combs, A. Yildiz, 'Cytoplasmic Dynein Moves Through Uncoordinated Stepping of the AAA+ Ring Domains', *Science*, **335**, 221–225 (2012). DOI: 10.1126/science.1215804
103. W. Qiu, N.D. Derr, B.S. Goodman, *et al.*, 'Dynein Achieves Processive Motion Using Both Stochastic and Coordinated Stepping', *Nat. Struct. Mol. Biol.*, **19**, 193–200 (2012). DOI: 10.1038/nsmb.2205
104. H.Y. Park, A.R. Buxbaum, R.H. Singer, 'Single mRNA Tracking in Live Cells', *Methods Enzymol.*, **472**, 387–406 (2010). DOI: 10.1016/S0076-6879(10)72003-6
105. H.Y. Park, H. Lim, Y.J. Yoon, *et al.*, 'Visualization of Dynamics of Single Endogenous mRNA Labeled in Live Mouse', *Science*, **343**, 422–424 (2014). DOI: 10.1126/science.1239200
106. A.R. Buxbaum, B. Wu, R.H. Singer, 'Single Beta-actin mRNA Detection in Neurons Reveals a Mechanism for Regulating its Translatability', *Science*, **343**, 419–422 (2014). DOI: 10.1126/science.1242939
107. T. Lohmuller, L. Iversen, M. Schmidt, *et al.*, 'Single Molecule Tracking on Supported Membranes With Arrays of Optical Nanoantennas', *Nano Lett.*, **12**, 1717–1721 (2012). DOI: 10.1021/nl300294b
108. J. Elf, G.W. Li, X.S. Xie, 'Probing Transcription Factor Dynamics at the Single-molecule Level in a Living Cell', *Science*, **316**, 1191–1194 (2007). DOI: 10.1126/science.1141967
109. A. Sanamrad, F. Persson, E.G. Lundius, *et al.*, 'Single-particle Tracking Reveals that Free Ribosomal Subunits are not Excluded from the Escherichia Coli Nucleoid', *Proc. Natl. Acad. Sci. U. S. A.*, (2014). DOI: 10.1073/pnas.1411558111
110. J.C. Gebhardt, D.M. Suter, R. Roy, *et al.*, 'Single-molecule Imaging of Transcription Factor Binding to DNA in Live Mammalian Cells', *Nat. Methods*, **10**, 421–426 (2013). DOI: 10.1038/nmeth.2411
111. J. Chen, Z. Zhang, L. Li, *et al.*, 'Single-molecule Dynamics of Enhanceosome Assembly in Embryonic Stem Cells', *Cell*, **156**, 1274–1285 (2014). DOI: 10.1016/j.cell.2014.01.062
112. M. Vrljic, S.Y. Nishimura, W.E. Moerner, 'Single-molecule Tracking', *Methods Mol. Biol.*, **398**, 193–219 (2007). DOI: 10.1007/978-1-59745-513-8_14
113. S. Wieser, G.J. Schutz, 'Tracking Single Molecules in the Live Cell Plasma Membrane-Do's and Don't's', *Methods*, **46**, 131–140 (2008). DOI: 10.1016/j.ymeth.2008.06.010
114. D. Shu, H. Zhang, J. Jin, P. Guo, 'Counting of six pRNAs of phi29 DNA-Packaging Motor With Customized Single-molecule Dual-view System', *EMBO J.*, **26**, 527–537 (2007). DOI: 10.1038/sj.emboj.7601506
115. K. Nakajo, M.H. Ulbrich, Y. Kubo, E.Y. Isacoff, 'Stoichiometry of the KCNQ1 – KCNE1 Ion Channel Complex', *Proc. Natl. Acad. Sci. U. S. A.*, **107**, 18862–18867 (2010). DOI: 10.1073/pnas.1010354107
116. H. Zhang, P. Guo, 'Single Molecule Photobleaching (SMPB) Technology for Counting of RNA, DNA, Protein and Other Molecules in Nanoparticles and Biological Complexes by TIRF Instrumentation', *Methods*, **67**, 169–176 (2014). DOI: 10.1016/j.ymeth.2014.01.010
117. N. Durisic, A.G. Godin, C.M. Wever, *et al.*, 'Stoichiometry of the human glycine receptor revealed by direct

Encyclopedia of Analytical Chemistry, Online © 2006–2015 John Wiley & Sons, Ltd.

This article was published in the *Encyclopedia of Analytical Chemistry* in 2015 by John Wiley & Sons, Ltd.
DOI: 10.1002/9780470027318.a9494

subunit counting', *J. Neurosci.: Off. J. Soc. Neurosci.*, **32**, 12915–12920 (2012). DOI: 10.1523/JNEUROSCI.2050-12.2012

118. A. Benke, N. Olivier, J. Gunzenhauser, S. Manley, 'Multicolor Single Molecule Tracking of Stochastically Active Synthetic Dyes', *Nano Lett.*, **12**, 2619–2624 (2012). DOI: 10.1021/nl301018r
119. A. Jain, R. Liu, Y.K. Xiang, T. Ha, 'Single-molecule Pull-down for Studying Protein Interactions', *Nat. Protoc.*, **7**, 445–452 (2012). DOI: 10.1038/nprot.2011.452
120. D.M. Rissin, C.W. Kan, T.G. Campbell, *et al.*, 'Single-molecule Enzyme-linked Immunosorbent Assay Detects Serum Proteins at Subfemtomolar Concentrations', *Nat. Biotechnol.*, **28**, 595–599 (2010). DOI: 10.1038/nbt.1641
121. M.H. Ulbrich, E.Y. Isacoff, 'Subunit Counting in Membrane-Bound Proteins', *Nat. Methods*, **4**, 319–321 (2007). DOI: 10.1038/nmeth1024
122. M.H. Ulbrich, E.Y. Isacoff, 'Rules of Engagement for NMDA Receptor Subunits', *Proc. Natl. Acad. Sci. U. S. A.*, **105**, 14163–14168 (2008). DOI: 10.1073/pnas.0802075105
123. L. Cai, N. Friedman, X.S. Xie, 'Stochastic Protein Expression in Individual Cells at the Single Molecule Level', *Nature*, **440**, 358–362 (2006). DOI: 10.1038/nature04599
124. X.S. Xie, P.J. Choi, G.W. Li, N.K. Lee, G. Lia, 'Single-molecule Approach to Molecular Biology in Living Bacterial Cells', *Annu. Rev. Biophys.*, **37**, 417–444 (2008). DOI: 10.1146/annurev.biophys.37.092607.174640
125. Y. Taniguchi, P. Choi, J.W. Li, *et al.*, 'Quantifying E. coli Proteome and Transcriptome With Single-molecule Sensitivity in Single Cells', *Science*, **329**, 533–538 (2010). DOI: 10.1126/science.1188308
126. R. Reyes-Lamothe, D.J. Sherratt, M.C. Leake, 'Stoichiometry and Architecture of Active DNA Replication Machinery in Escherichia Coli', *Science*, **328**, 498–501 (2010). DOI: 10.1126/science.1185757
127. M. Plank, G.H. Wadhams, M.C. Leake, 'Millisecond Timescale Slimfield Imaging and Automated Quantification of Single Fluorescent Protein Molecules for Use in Probing Complex Biological Processes', *Integr. Biol.: Quant. Biosci. Nano Macro*, **1**, 602–612 (2009). DOI: 10.1039/b907837a
128. A. Badrinarayanan, C. Lesterlin, R. Reyes-Lamothe, D. Sherratt, 'The Escherichia coli SMC Complex, MukBEF, Shapes Nucleoid Organization Independently of DNA Replication', *J. Bacteriol.*, **194**, 4669–4676 (2012). DOI: 10.1128/JB.00957-12
129. K.I. Willig, B. Harke, R. Medda, S.W. Hell, 'STED Microscopy with Continuous Wave Beams', *Nat. Methods*, **4**, 915–918 (2007). DOI: 10.1038/nmeth1108
130. L. Schermelleh, P.M. Carlton, S. Haase, *et al.*, 'Subdiffraction Multicolor Imaging of the Nuclear Periphery With 3D Structured Illumination Microscopy', *Science*, **320**, 1332–1336 (2008). DOI: 10.1126/science.1156947
131. B. Harke, J. Keller, C.K. Ullal, *et al.*, 'Resolution Scaling in STED Microscopy', *Opt. Express*, **16**, 4154–4162 (2008).
132. M.G. Gustafsson, L. Shao, P.M. Carlton, *et al.*, 'Three-dimensional Resolution Doubling in Wide-field Fluorescence Microscopy by Structured Illumination', *Biophys. J.*, **94**, 4957–4970 (2008). DOI: 10.1529/biophysj.107.120345
133. E. Betzig, G.H. Patterson, R. Souqurat, *et al.*, 'Imaging Intracellular Fluorescent Proteins at Nanometer Resolution', *Science*, **313**, 1642–1645 (2006). DOI: 10.1126/science.1127344
134. M.J. Rust, M. Bates, X. Zhuang, 'Sub-diffraction-limit Imaging by Stochastic Optical Reconstruction Microscopy (STORM)', *Nat. Methods*, **3**, 793–795 (2006). DOI: 10.1038/nmeth929
135. S. van de Linde, S. Wolter, M. Heilemann, M. Sauer, 'The Effect of Photoswitching Kinetics and Labeling Densities on Super-resolution Fluorescence Imaging', *J. Biotechnol.*, **149**, 260–266 (2010). DOI: 10.1016/j.jbiotec.2010.02.010
136. D. Greenfield, A.L. McEvoy, H. Shroff, *et al.*, 'Self-organization of the Escherichia Coli Chemotaxis Network Imaged With Super-resolution Light Microscopy', *PLoS Biol.*, **7**, e1000137 (2009). DOI: 10.1371/journal.pbio.1000137
137. G.T. Dempsey, J.C. Vaughan, K.H. Chen, M. Bates, X. Zhuang, 'Evaluation of Fluorophores for Optimal Performance in Localization-based Super-resolution Imaging', *Nat. Methods*, **8**, 1027–1036 (2011). DOI: 10.1038/nmeth.1768
138. S. van de Linde, A. Löschberger, T. Klein, *et al.*, 'Direct Stochastic Optical Reconstruction Microscopy with Standard Fluorescent Probes', *Nat. Protoc.*, **6**, 991–1009 (2011). DOI: 10.1038/nprot.2011.336
139. N. Durisic, L. Laparra-Cuervo, A. Sandoval-Alvarez, J.S. Borbely, M. Lakadamyali, 'Single-molecule Evaluation of Fluorescent Protein Photoactivation Efficiency Using an in Vivo Nanotemplate', *Nat. Methods*, **11**, 156–162 (2014). DOI: 10.1038/nmeth.2784
140. F.V. Subach, G.H. Patterson, S. Manley, *et al.*, 'Photoactivatable mCherry for High-resolution two-color Fluorescence Microscopy', *Nat. Methods*, **6**, 153–159 (2009). DOI: 10.1038/nmeth.1298
141. H. Shroff, C.G. Galbraith, J.A. Galbraith, *et al.*, 'Dual-color Superresolution Imaging of Genetically Expressed Probes Within Individual Adhesion Complexes', *Proc. Natl. Acad. Sci. U. S. A.*, **104**, 20308–20313 (2007). DOI: 10.1073/pnas.0710517105
142. S. van de Linde, H. Rainer, L. Heinirch, *et al.*, 'Multicolor Photoswitching Microscopy for Subdiffraction-resolution Fluorescence Imaging', *Photochem. Photobiol. Sci.: Off. J. Eur. Photochem. Assoc. Eur. Soc. Photobiol.*, **8**, 465–469 (2009). DOI: 10.1039/b822533h
143. Y.S. Hu, X. Nan, P. Sengupta, J. Lippincott-Schwartz, H. Cang, 'Accelerating 3B Single-molecule Super-resolution

Encyclopedia of Analytical Chemistry, Online © 2006–2015 John Wiley & Sons, Ltd.

This article was published in the *Encyclopedia of Analytical Chemistry* in 2015 by John Wiley & Sons, Ltd.
DOI: 10.1002/9780470027318.a9494

Microscopy with Cloud Computing', *Nat. Methods*, **10**, 96–97 (2013). DOI: 10.1038/nmeth.2335

144. P. Sengupta, T. Jovanovic-Talisman, J. Lippincott-Schwartz, 'Quantifying Spatial Organization in Point-localization Superresolution Images Using Pair Correlation Analysis', *Nat. Protoc.*, **8**, 345–354 (2013). DOI: 10.1038/nprot.2013.005
145. T. Dertinger, R. Colyer, G. Iyer, S. Weiss, J. Enderlein, 'Fast, Background-free, 3D Super-resolution Optical Fluctuation Imaging (SOFI)', *Proc. Natl. Acad. Sci. U. S. A.*, **106**, 22287–22292 (2009). DOI: 10.1073/pnas.0907866106
146. T. Dertinger, A. Pallaoro, G. Braun, *et al.*, 'Advances in Superresolution Optical Fluctuation Imaging (SOFI)', *Q. Rev. Biophys.*, **46**, 210–221 (2013). DOI: 10.1017/S0033583513000036
147. S.J. Holden, S. Uphoff, A.N. Kapanidis, 'DAOSTORM: An algorithm for High- Density Super-Resolution Microscopy', *Nat. Methods*, **8**, 279–280 (2011). DOI: 10.1038/nmeth0411-279
148. A. Szymborska, A. de Marco, N. Daigle, *et al.*, 'Nuclear Pore Scaffold Structure Analyzed by Super-resolution Microscopy and Particle Averaging', *Science*, **341**, 655–658 (2013). DOI: 10.1126/science.1240672
149. V. Mennella, B. Keszthelvi, K.L. McDonald, *et al.*, 'Subdiffraction-resolution Fluorescence Microscopy Reveals a Domain of the Centrosome Critical for Pericentriolar Material Organization', *Nat. Cell Biol.*, **14**, 1159–1168 (2012). DOI: 10.1038/ncb2597
150. S. Lawo, M. Hasegan, G.D. Gupta, L. Pelletier, 'Subdiffraction Imaging of Centrosomes Reveals Higher-order Organizational Features of Pericentriolar Material', *Nat. Cell Biol.*, **14**, 1148–1158 (2012). DOI: 10.1038/ncb2591
151. Y. Hou, D.J. Crossman, V. Rajagopal, *et al.*, 'Super-resolution Fluorescence Imaging to Study Cardiac Biophysics: Alpha-actinin Distribution and Z-disk Topologies in Optically Thick Cardiac Tissue Slices', *Prog. Biophys. Mol. Biol.*, (2014). DOI: 10.1016/j.pbiomolbio.2014.07.003
152. E.C. Friedberg, 'DNA Damage and Repair', *Nature*, **421**, 436–440 (2003). DOI: 10.1038/nature01408
153. B. Huang, S.A. Jones, B. Brandenburg, X. Zhuang, 'Whole-cell 3D STORM Reveals Interactions Between Cellular Structures With Nanometer-scale Resolution', *Nat. Methods*, **5**, 1047–1052 (2008). DOI: 10.1038/nmeth.1274
154. M. Lakadamyali, H. Babcock, M. Bates, X. Zhuang, J. Lichtman, '3D Multicolor Super-resolution Imaging Offers Improved Accuracy in Neuron Tracing', *PLoS One*, **7**, e30826 (2012). DOI: 10.1371/journal.pone.0030826
155. A. Dani, B. Huang, J. Bergan, C. Dulac, X. Zhuang, 'Superresolution Imaging of Chemical Synapses in the Brain', *Neuron*, **68**, 843–856 (2010). DOI: 10.1016/j.neuron.2010.11.021
156. S.J. Holden, T. Pengo, K.L. Meibom, *et al.*, 'High Throughput 3D Super-resolution Microscopy Reveals Caulobacter Crescentus in Vivo Z-ring Organization', *Proc. Natl. Acad. Sci. U. S. A.*, **111**, 4566–4571 (2014). DOI: 10.1073/pnas.1313368111
157. G. Shtengel, J.A. Galbraith, C.G. Galbraith, *et al.*, 'Interferometric Fluorescent Super-resolution Microscopy Resolves 3D Cellular Ultrastructure', *Proc. Natl. Acad. Sci. U. S. A.*, **106**, 3125–3130 (2009). DOI: 10.1073/pnas.0813131106
158. P. Kanchanawong, G. Shtengel, A.M. Pasapera, *et al.*, 'Nanoscale Architecture of Integrin-based Cell Adhesions', *Nature*, **468**, 580–584 (2010). DOI: 10.1038/nature09621
159. Y. Wang, G. Fruhwirth, E. Cai, T. Ng, P.R. Selvin, '3D Super-resolution Imaging With Blinking Quantum Dots', *Nano Lett.*, **13**, 5233–5241 (2013). DOI: 10.1021/nl4026665
160. N. Olivier, D. Keller, P. Gonczy, S. Manley, 'Resolution Doubling in 3D-STORM Imaging Through Improved Buffers', *PLoS One*, **8**, e69004 (2013). DOI: 10.1371/journal.pone.0069004
161. K. Klehs, K. Klehs, K. Klehs, *et al.*, 'Increasing the Brightness of Cyanine Fluorophores for Single-molecule and Superresolution Imaging', *Chemphyschem: Eur. J. Chem. Phys. Phys. Chem.*, **15**, 637–641 (2014). DOI: 10.1002/cphc.201300874
162. K. Xu, H.P. Babcock, X. Zhuang, 'Dual-objective STORM Reveals Three-dimensional Filament Organization in the Actin Cytoskeleton', *Nat. Methods*, **9**, 185–188 (2012). DOI: 10.1038/nmeth.1841
163. A. Pertsinidis, Y. Zhang, S. Chu, 'Subnanometre Single-molecule Localization, Registration and Distance Measurements', *Nature*, **466**, 647–651 (2010). DOI: 10.1038/nature09163
164. R. Henriques, M. Lelek, E.F. Fornasiero, *et al.*, 'QuickPALM: 3D Real-time Photoactivation Nanoscopy Image Processing in ImageJ', *Nat. Methods*, **7**, 339–340 (2010). DOI: 10.1038/nmeth0510-339
165. A.G. York, A. Ghitani, A. Vaziri, M.W. Davidson, H. Shroff, 'Confined Activation and Subdiffractive Localization Enables Whole-cell PALM With Genetically Expressed Probes', *Nat. Methods*, **8**, 327–333 (2011). DOI: 10.1038/nmeth.1571
166. M. Ovesny, P. Krizek, J. Borkovec, Z. Svindrych, G.M. Hagen, 'ThunderSTORM: a Comprehensive ImageJ plug-in for PALM and STORM Data Analysis and Super-resolution Imaging', *Bioinformatics*, (2014). DOI: 10.1093/bioinformatics/btu202
167. S. Wolter, A. Löschberger, T. Holm, *et al.*, 'rapidSTORM: Accurate, Fast Open-source Software for Localization Microscopy', *Nat. Methods*, **9**, 1040–1041 (2012). DOI: 10.1038/nmeth.2224

Encyclopedia of Analytical Chemistry, Online © 2006–2015 John Wiley & Sons, Ltd.

This article was published in the *Encyclopedia of Analytical Chemistry* in 2015 by John Wiley & Sons, Ltd.
DOI: 10.1002/9780470027318.a9494

168. N. Durisic, L.L. Cuervo, M. Lakadamyali, 'Quantitative Super-resolution Microscopy: Pitfalls and Strategies for Image Analysis', *Curr. Opin. Chem. Biol.*, **20C**, 22–28 (2014). DOI: 10.1016/j.cbpa.2014.04.005

169. K.W. Dunn, M.M. Kamocka, J.H. McDonald, 'A Practical Guide to Evaluating Colocalization in Biological Microscopy', *Am. J. Physiol. Cell Physiol.*, **300**, C723–C742 (2011). DOI: 10.1152/ajpcell.00462.2010

170. E. Agullo-Pascual, D.A. Reid, S. Keegan, *et al.*, 'Super-resolution Fluorescence Microscopy of the Cardiac Connexome Reveals Plakophilin-2 Inside the Connexin43 Plaque', *Cardiovasc. Res.*, **100**, 231–240 (2013). DOI: 10.1093/cvr/cvt191

171. I.D. Jayasinghe, D. Baddeley, C.H. Kong, *et al.*, 'Nanoscale Organization of Junctophilin-2 and Ryanodine Receptors Within Peripheral Couplings of Rat Ventricular Cardiomyocytes', *Biophys. J.*, **102**, L19–L21 (2012). DOI: 10.1016/j.bpj.2012.01.034

172. C. Soeller, D. Baddeley, 'Super-resolution Imaging of EC Coupling Protein Distribution in the Heart', *J. Mol. Cell. Cardiol.*, **58**, 32–40 (2013). DOI: 10.1016/j.yjmcc.2012.11.004

173. J. Wong, D. Baddeley, E.A. Bushong, *et al.*, 'Nanoscale Distribution of Ryanodine Receptors and Caveolin-3 in Mouse Ventricular Myocytes: Dilation of t-tubules Near Junctions', *Biophys. J.*, **104**, L22–L24 (2013). DOI: 10.1016/j.bpj.2013.02.059

174. X. Nan, E.A. Collission, S. Lewis, *et al.*, 'Single-molecule Superresolution Imaging Allows Auantitative Analysis of RAF Multimer Formation and Signaling', *Proc. Natl. Acad. Sci. U. S. A.*, **110**, 18519–18524 (2013). DOI: 10.1073/pnas.1318188110

175. J. Eid, A. Fehr, J. Gray, *et al.*, 'Real-time DNA Sequencing from Single Polymerase Molecules', *Science*, **323**, 133–138 (2009). DOI: 10.1126/science.1162986

176. J. Korlach, A. Bibillo, J. Wegener, *et al.*, 'Long, Processive Enzymatic DNA Synthesis Using 100% Dye-labeled Terminal Phosphate-linked Nucleotides', *Nucleosides Nucleotides Nucleic Acids*, **27**, 1072–1083 (2008). DOI: 10.1080/15257770802260741

177. P. Holzmeister, G.P. Acuna, D. Grohmann, P. Tinnefeld, 'Breaking the Concentration Limit of Optical Single-molecule Detection', *Chem. Soc. Rev.*, **43**, 1014–1028 (2014). DOI: 10.1039/c3cs60207a

178. M.J. Levene, J. Korlach, S. Turner, *et al.*, 'Zero-mode Waveguides for Single-molecule Analysis at High Concentrations', *Science*, **299**, 682–686 (2003). DOI: 10.1126/science.1079700

179. P.M. Lundquist, C.F. Zhong, P. Zhao, *et al.*, 'Parallel Confocal Detection of Single Molecules in Real Time', *Opt. Lett.*, **33**, 1026–1028 (2008).

180. J. Chen, R.V. Dalal, A.N. Petroy, *et al.*, 'High-throughput Platform for Real-time Monitoring of Biological Processes by Multicolor Single-molecule Fluorescence', *Proc. Natl. Acad. Sci. U. S. A.*, **111**, 664–669 (2014). DOI: 10.1073/pnas.1315735111

181. N.G. Walter, 'Future of Biomedical Sciences: Single Molecule Microscopy', *Biopolymers*, **85**, 103–105 (2007). DOI: 10.1002/Bip.20633

182. S. Cho, J. Jang, C. Song, *et al.*, 'Simple Super-resolution Live-cell Imaging Based on Diffusion-assisted Forster Resonance Energy Transfer', *Sci. Rep.*, **3**, 1208 (2013). DOI: 10.1038/srep01208

183. G. Shtengel, Y. Wang, Z. Zhang, *et al.*, 'Imaging Cellular Ultrastructure by PALM, iPALM, and correlative iPALM-EM', *Methods Cell Biol.*, **123**, 273–294 (2014). DOI: 10.1016/B978-0-12-420138-5.00015-X

184. B.G. Kopek, G. Shtengel, J.B. Grimm, D.A. Clayton, H.F. Hess, 'Correlative Photoactivated Localization and Scanning Electron Microscopy', *PLoS One*, **8**, e77209 (2013). DOI: 10.1371/journal.pone.0077209

185. S.C. Pavlides, K.T. Huang, D.A. Reid, *et al.*, 'Inhibitors of SCF-Skp2/Cks1 E3 Ligase Block Estrogen-induced Growth Stimulation and Degradation of Nuclear p27kip1: Therapeutic Potential for Endometrial Cancer', *Endocrinology*, **154**, 4030–4045 (2013). DOI: 10.1210/en.2013-1757

186. M. Johansson, J. Chen, A. Tsai, G. Kornberg, J.D. Puglisi, 'Sequence-dependent Elongation Dynamics on Macrolide-bound Ribosomes', *Cell Reports*, **7**, 1534–1546 (2014). DOI: 10.1016/j.celrep.2014.04.034

187. E.C. Greene, S. Wind, T. Fazio, J. Gorman, M.L. Visnapuu, 'DNA Curtains for High-throughput Single-molecule Optical Imaging', *Methods Enzymol.*, **472**, 293–315 (2010). DOI: 10.1016/S0076-6879(10)72006-1

Encyclopedia of Analytical Chemistry, Online © 2006–2015 John Wiley & Sons, Ltd.

This article was published in the *Encyclopedia of Analytical Chemistry* in 2015 by John Wiley & Sons, Ltd.
DOI: 10.1002/9780470027318.a9494